flow (PEF) in asthmatics.[9] However, when patients with comorbid AR were evaluated, the addition of LM was significantly better at improving airflow limitation than doubling the dose of ICS.[10] These results suggest that the addition of LM to ICS could be useful in treating asthmatics whose asthma is not well controlled with steroid therapy, especially in patients comorbid with AR. Although the additive anti-inflammatory properties of LM in asthmatics receiving steroid therapy have been examined using sputum eosinophil counting and exhaled nitric oxide measurements,[11-13] little is known about its molecular mechanism of action.

In the present study, we evaluated the additive effects of LM with ICS on pulmonary function and airway cytokine expression in asthmatics with or without AR. Furthermore, the relationship between the changes in the molecule expression and the physiological properties of asthma, such as airflow limitation and airway lability, was examined.

METHODS

STUDY SUBJECTS

Eighteen uncontrolled steroid-treated asthmatics, nine with AR and nine without AR, were enrolled in a randomized fashion after giving informed consent. To avoid the influence of the pollen season, the enrollment was performed from May to September 2006. The study was approved by the local ethics committee. All patients satisfied the American Thoracic Society criteria for asthma.[14] Patients with rhinitis were identified by specialists. All patients were receiving inhaled steroid therapy (equivalent dose of 400 μg fluticasone · day^{-1}) and used inhaled short acting β_2 agonists as needed for symptom relief. Subjects were not included if they had had an exacerbation of asthma or a respiratory tract infection in the 2 weeks preceding the examination.

STUDY DESIGN

On the first day, spirometry and exhaled breath condensate (EBC) collections were performed. PEF monitoring had been started at least 4 weeks before this examination. After assessment of the baseline values, open, uncontrolled LM therapy (asthma with AR group, pranlukast in 5 cases and montelukast in 4 cases; asthma without AR group, pranlukast in 4 cases and montelukast in 5 cases) was administered for 8 weeks, and then the same examination was repeated.

EBC COLLECTION

EBC collection was performed with a standardized method according to the recommended procedure.[15] The EBC was collected by using a condenser, which permitted noninvasive collection of condensed exhaled air by freezing it to -20℃ (Ecoscreen; Jaeger, Hoechberg, Germany). The subjects breathed through a mouthpiece and a two-way non-rebreathing valve, which also served as a saliva trap. Subjects were asked to breath at a normal frequency and tidal volume while wearing a nose-clip. The collected EBC was stored at -70℃ and cytokine measurements were performed within 4 weeks.

Table 1 Subject demographics

	Asthma/AR +	Asthma/AR −
Number	9 (F/M = 6/3)	9 (F/M = 4/5)
Age (years)	42.3 ± 6.5	43.0 ± 4.6
FVC (L)	3.27 ± 0.26	3.72 ± 0.24
FEV_1 (L)	2.47 ± 0.24	2.75 ± 0.21
FEV_1% (%)	74.8 ± 3.8	73.8 ± 2.9
%FEV_1 (%)	84.6 ± 4.6	86.2 ± 3.6
Min%MaxPEF (%)	82.6 ± 2.1	84.4 ± 2.2

Definition of abbreviations: AR, allergic rhinitis; F, female; M, male; FVC, forced vital capacity; FEV_1, forced expiratory volume in one second; PEF, peak expiratory flow; Min%Max PEF, the lowest PEF over a week expressed as % highest PEF. Values are means ± SE.

CYTOKINE MEASUREMENTS

Human Inflammation Antibody III (Ray Biotech Inc., Norcross, GA, USA), consisting of 40 different cytokine and chemokine antibodies spotted in duplicate onto a membrane, was utilized as previously described.[16] The intensity of the signals was detected directly from the membranes using a chemiluminescene imaging system (Luminocapture AE6955; Atto Co., Tokyo, Japan). HRP-conjugated antibody served as a positive control at six spots and was also used to identify the membrane orientation. For each spot, the net intensity gray level was determined by subtracting the background gray levels from the total raw intensity gray levels. The relative intensity levels of the cytokine amounts were normalized with reference to the amount present on the positive control in each membrane on the following basis: average of the cytokine spot intensities/average of the positive control spot intensities, indicated as a percentage. Using this technique, we have previously shown that the expressions of IL-4, IL-17, RANTES, MIP-1α, MIP-1β, IP-10, IL-8, TNF-α, and TGF-β were increased in asthmatic airways.[16] Thus, these nine cytokines were selected as target molecules.

PEAK EXPIRATORY FLOW (PEF) MEASUREMENTS

PEF was measured using an Assess® peak flow meter (Respironics HealthScan Co., NJ, USA). Among PEF indices, the lowest PEF over a week, expressed as a percentage of the highest PEF (Min%Max PEF), has been suggested to be the best index of airway lability.[17] We have confirmed that Min%Max PEF showed a good correlation with the degree of airway

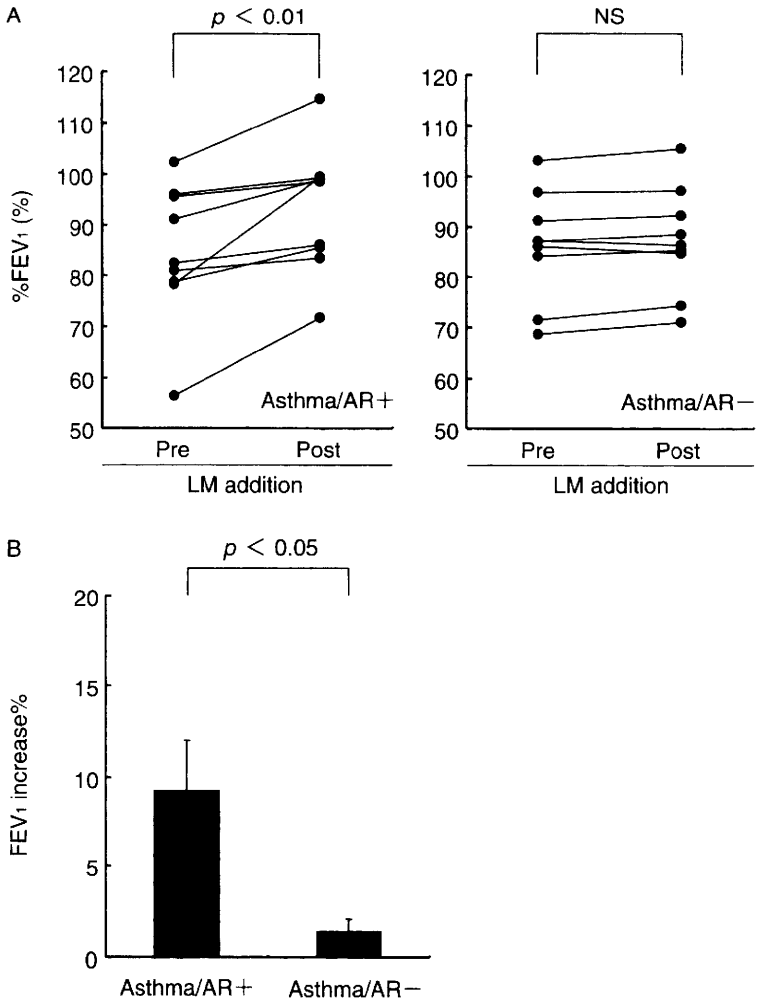

Fig. 1 Graphs of individual forced expiratory volume in one second (FEV_1) at baseline and at the end of additive leukotriene modifier (LM) therapy in asthma patients with or without allergic rhinitis (AR) (**A**), and mean change from baseline in FEV_1 for each subgroup (**B**).

hyperresponsiveness (AHR) measured by the inhalation challenge test,[18] and thus Min%Max PEF was used as an index of fluctuation of the airway caliber in this study.

PULMONARY FUNCTION TEST

Forced expiratory volume in one second (FEV_1) and forced vital capacity (FVC) were measured with a Vitalograph Pneumotrac 6800™ (Vitarograph Co., Ennis, Ireland).

STATISTICAL ANALYSES

Comparisons of before and after LM therapy were performed by Mann-Whitney *U* tests and comparisons between groups were performed by Fisher's exact tests. Pearson's correlation coefficients were calculated to determine the correlation between the changes in the levels of cytokine expression and pulmonary physiological parameters by LM therapy. All data were expressed as means ± SE, and significance was defined as a *P* value of less than 0.05.

RESULTS

SUBJECT DEMOGRAPHICS

The clinical characteristics of the study subjects are shown in Table 1. There were no significant differences in baseline characteristics between the groups. The asthma control levels of all subjects were classified as partly controlled at baseline.[19] After LM additive therapy, asthma symptoms in seven of nine asthmatics with AR and five of nine asthmatics without AR were improved to a controlled level. The rates of improvement were higher in the asthma with AR group, but the differences were not significant. There were no subjects whose asthma control levels worsened. All of the asthma with AR subjects had nasal

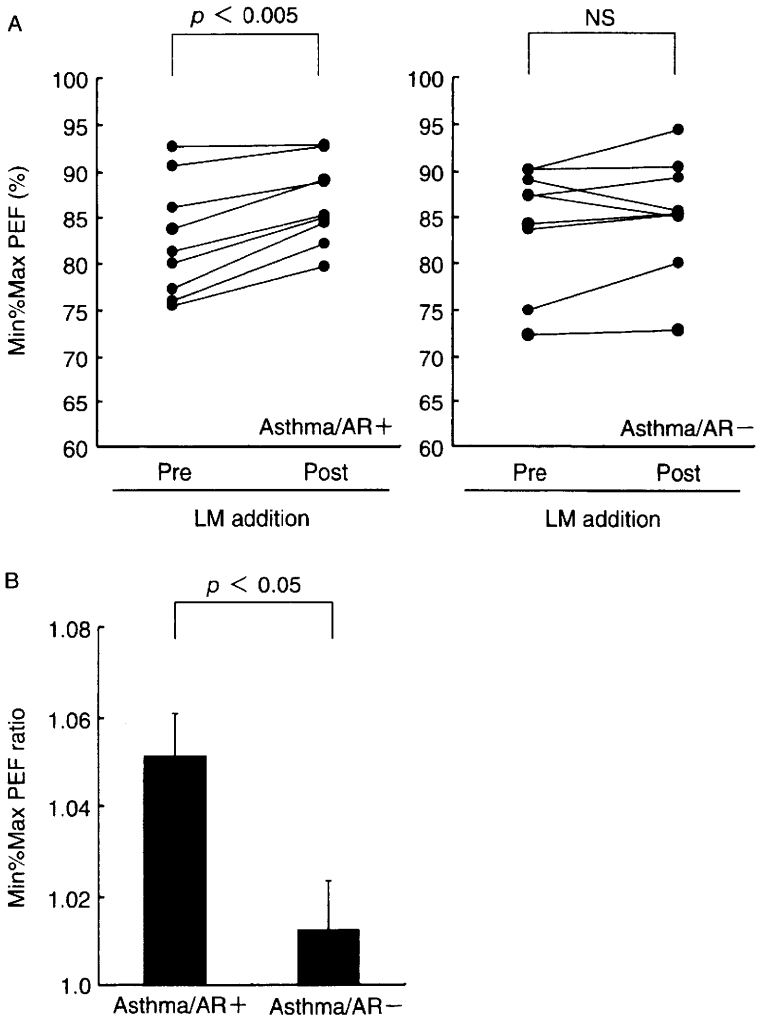

Fig. 2 Graphs of individual peak expiratory flow (PEF) variability (Min%Max PEF) at baseline and at the end of additive leukotriene modifier (LM) therapy in asthma patients with or without allergic rhinitis (AR) (**A**), and mean changes from baseline in Min%Max PEF for each subgroup (**B**).

symptoms at baseline; there was nasal discharge in seven subjects and nasal blockage in four subjects. Additive LM improved the nasal discharge in four subjects and nasal blockage in three subjects.

PULMONARY FUNCTION

A significant improvement in the parameter that represents airway caliber, FEV_1 as a percentage of the predicted value (%FEV_1), was seen in the subgroup of asthma with AR by additive LM therapy (Fig. 1A, B). LM therapy also improved the parameters that represent airway lability, Min%Max PEF, in the asthma with AR group but not in the asthma without AR group (Fig. 2A, B). The kind of LM used was not related to the additive effects on pulmonary function. The LM-mediated improvement in airflow limitation, namely the increase in %FEV_1, was significantly correlated with the changes of Min%Max PEF ($r = 0.754$, $p < 0.01$, [Fig. 3]).

AIRWAY CYTOKINE EXPRESSION

There was no significant difference in the baseline cytokine values between the two groups (Fig. 4). Among the nine examined molecules, the RANTES level in the asthma with AR group was significantly reduced by LM therapy ($p < 0.05$), whereas there were no significant changes in all examined cytokine levels in the asthma without AR group (Fig. 5A, B). The kind of LM used was not related to the changes in the cytokine expressions by LM additive therapy.

RELATIONSHIP BETWEEN CHANGES IN RANTES LEVELS AND PULMONARY PHYSIOLOGICAL PARAMETERS BY ADDITIVE LM THERAPY

The changes in the RANTES levels by additive LM therapy were significantly correlated with the im-

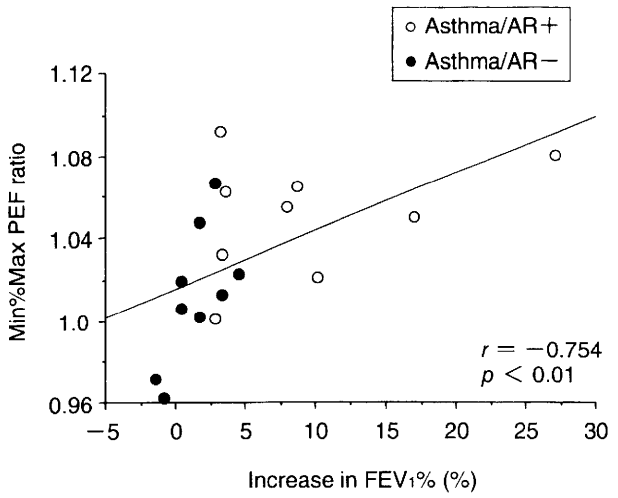

Fig. 3 Relationship between leukotriene modifier-mediated improvement in forced expiratory in one second and peak expiratory flow variability in asthma patients with (open circles) or without (closed circles) allergic rhinitis (AR). The lines correspond to the fitted regression equation.

provement in the FEV_1 increase% and the ratio of Min %Max PEF ($r = -0.736$, $p < 0.01$, Fig. 6A and $r = -0.622$, $p < 0.05$, Fig. 6B, respectively). Correlations between LM-mediated changes in the levels of other molecules and the physiologic properties were not seen.

DISCUSSION

In the present study, adding LM therapy to ICS improved the airflow limitation and airway lability, and improvement was significant in the subgroup of asthma with AR but not in the asthma without AR group. There was no significant difference in the baseline cytokine values between the groups. However, the exhaled RANTES levels were significantly reduced by LM in the asthma with AR group. The changes in the RANTES level were related to the changes in the physiologic properties, such as $\%FEV_1$ and Min%Max PEF values.

To our knowledge, the current report is the first direct comparison study to evaluate the additive effect of LM on pulmonary function and airway cytokine expression between steroid-treated asthmatics with AR and those without AR. Asthma and AR often co-exist and upper airway diseases can influence lower airway inflammation and function in some patients with asthma.[1] Allergen challenge to the lung leads to inflammation in the nose.[20] Similarly, allergen challenge to the nose leads to AHR in the lower airway.[21] CysLTs are key mediators and modulators of systemic allergic responses as well as a component of the inflammatory responses that lead to the typical symptoms of asthma and rhinitis.[2] CysLTs facilitate eosinophil recruitment into susceptible tissues and prolong their survival, contributing to the maintenance of the inflammatory reaction.[22] In addition, CysLTs have modulating effects on the cytokine activity and production from cells.[2] A previous study has shown that CysLTs stimulate lung mononuclear cells to release inflammatory mediators, such as RANTES.[23] Allergen challenge induces RANTES positive cells in accordance with increased eosinophils in the airway, and LM suppresses airway eosinophils and RANTES production.[24,25] These studies show that LM has the potential to suppress airway RANTES expression by the blockage of CysLTs.

In this study, LM provided significant improvements in airflow limitation in asthmatics with AR, in agreement with a previous study.[10] In addition, we are the first to demonstrate that LM causes a greater improvement in pulmonary function and exhaled RANTES expression in asthmatics with AR than in those without AR. Although airway inflammation seems likely to play a similar role in the pathogenesis of AR as in asthma, it may be difficult to explain our results by the differences in the degree of airway inflammation between the two groups. Even in the absence of rhinitis, asthma patients have increased eosinophil levels in nasal mucosa, and these levels are related to the bronchial eosinophil values.[26] The present study also showed that the cytokine values at baseline were similar in the two groups.

Previous studies have shown that there is increased excretion of urinary leukotriene E4 in asthmatics with AR.[27] Nasal allergen challenge causes a dose-dependent increase in CysLTs that correlates with nasal symptoms.[28] In addition, the sputum CysLTs levels obtained from asthmatics remain elevated despite ICS treatment.[29] Consequently, despite receiving steroid therapy, CysLTs are over-expressed in the asthmatic airway and possibly more so in patients comorbid with AR. This speculation may explain the present result that LM significantly reduced the RANTES levels only in the asthma with AR group. However, the expression of CysLTs in the lower airways has not been directly compared between groups, although increased CysLT levels have been shown in the BAL fluid and sputum of patients with asthma.[29,30] In addition, in other previously proposed theories of the interaction between asthma and AR, the irritant effects of nasal secretions directly entering the lower airways and systemic propagation of nasal inflammation to the lower airways,[31] may be involved in the mechanism of the present result. However, the current study was not able to prove these possibilities.

The RANTES-mediated pathway may be involved in the improvements of the airflow limitation and airway lability by the addition of LM in asthmatics receiving steroid therapy. A possible explanation for this association may be as follows. In asthmatic airways, RANTES have a potent role in eosinophil re-

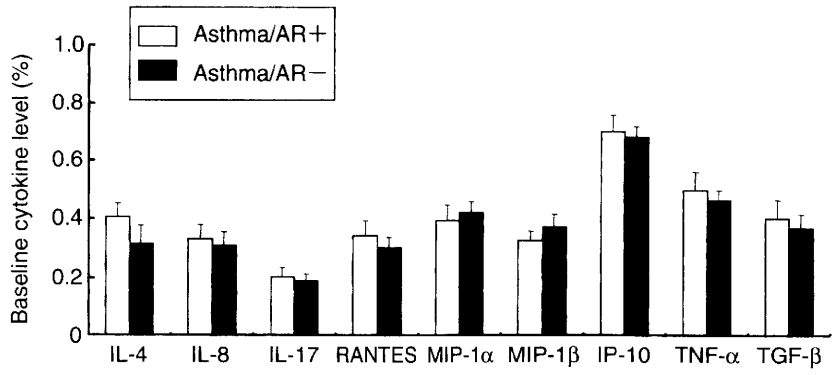

Fig. 4 Baseline expression levels of IL-4, IL-8, IL-17, RANTES, MIP-1α, MIP-1β, IP-10, TNF-α, and TGF-β in exhaled breath condensate obtained from asthma patients with (open bars) or without (filled bars) allergic rhinitis (AR).

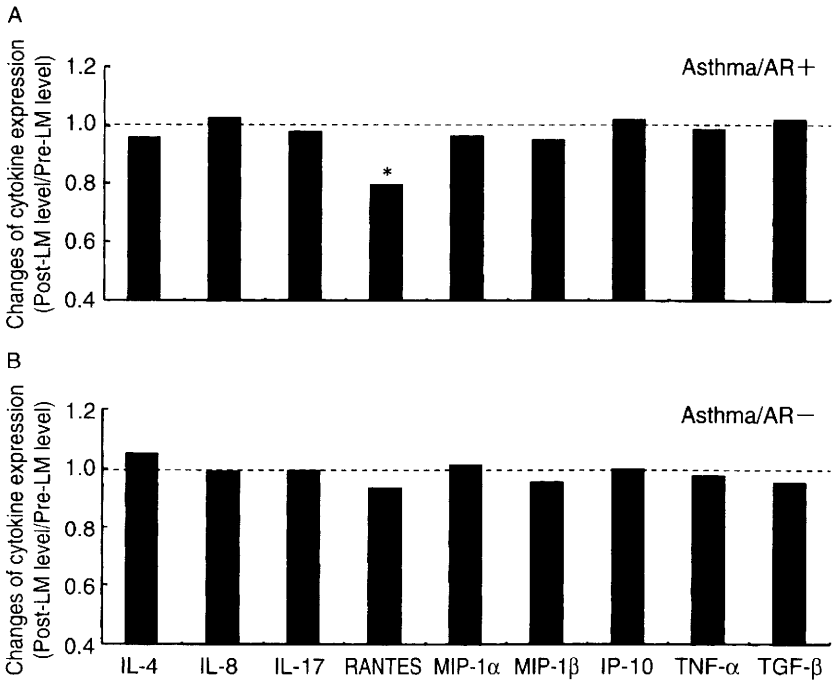

Fig. 5 Changes of expression levels of IL-4, IL-8, IL-17, RANTES, MIP-1α, MIP-1β, IP-10, TNF-α, and TGF-β in exhaled breath condensate by additive leukotriene modifier (LM) therapy in asthma patients with (**A**) or without (**B**) allergic rhinitis (AR). $*p < 0.05$ compared with baseline cytokine levels.

cruitment in the airway,[32,33] and RANTES-positive sputum eosinophils are correlated with the degree of %FEV_1 after allergen challenge.[33] LM therapy may modulate the cytokine expression, such as RANTES, with a consequent inhibition of the airway inflammation resulting in improvement of the pulmonary function. It has been shown that improvements in airflow limitation and AHR in asthmatics are accompanied by a decrease of airway inflammation and reduction in the RANTES expression,[33,34] which is compatible with our results.

Furthermore, RANTES activate immune cells and induce the exocytosis of bronchoconstrictive mediators resulting in airflow limitation.[32,33] Using a murine asthma model, a previous study has shown that the blockage of RANTES reduces AHR.[35] In the present study, the reduction in the exhaled RANTES levels was associated with improvements in both the airflow limitation and airway lability. The LM-mediated improvements in the airflow limitation were related to the changes in airway lability. These results suggest that LM can inhibit the airflow limitation induced by

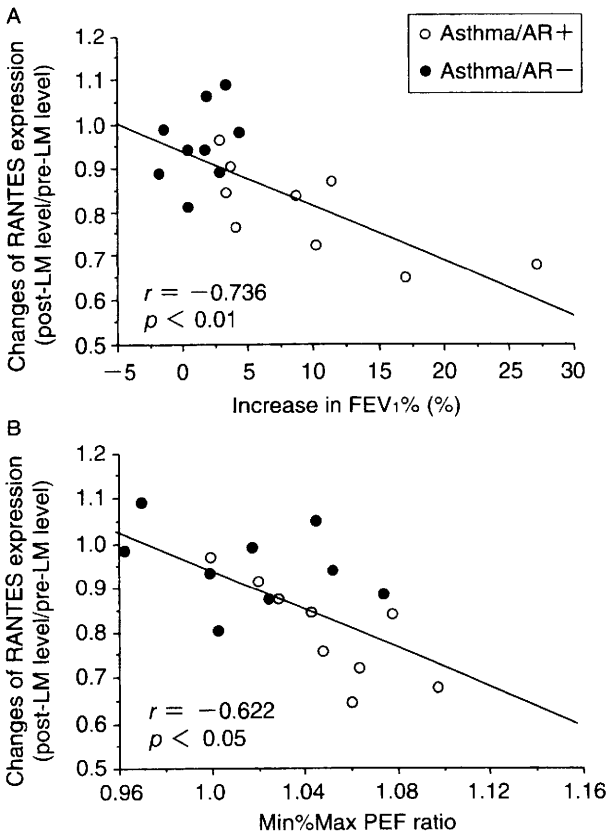

Fig. 6 Relationship between leukotriene modifier (LM)-mediated changes of RANTES expression (the ratio of post-LM level/pre-LM level) and improvement in physiological parameters: forced expiratory volume in one second (**A**) and peak expiratory flow variability (**B**) (open circles, asthma patients with allergic rhinitis [AR]; closed circles, asthma patients without AR). The lines correspond to the fitted regression equation.

RANTES and thereby improve the fluctuation of the airway caliber.

The limitations of the current study are as follows. The enrollment of subjects was carefully performed to avoid the influence of the pollen season. However, the possibility that the changes in the parameters could be attributed to a seasonal effect remained. Furthermore, the small number of study subjects may affect the result that LM did not significantly improve the examined parameters in the asthma without AR group. This report does not claim that LM should not be used for asthma without AR patients. Finally, this small-scaled study did not have enough power to examine the association between the LM-mediated changes in symptoms and RANTES levels in EBC.

In conclusion, LM caused a greater improvement in pulmonary function and airway inflammation in asthmatics with AR. The RANTES-mediated pathway may be involved in the improvement of the airflow limitation and airway lability by LM additive therapy in asthmatics receiving steroid therapy.

REFERENCES

1. Bousquet J, Van Cauwenberge P, Khaltaev N. Allergic rhinitis and its impact on asthma. *J Allergy Clin Immunol* 2001;**108**(Suppl 5):S147-34.
2. Busse WW, Kraft M. Cysteinyl leukotrienes in allergic inflammation: strategic target for therapy. *Chest* 2005;**127**: 1312-26.
3. Reiss TF, Chervinsky PS, Dockhorn RJ, Shingo S, Seidenberg B, Edwards TB. Montelukast, a once-daily leukotriene receptor antagonist, in the treatment of chronic asthma. *Arch Intern Med* 1998;**158**:1213-20.
4. Israel E, Chervinsky PS, Friedman B, Van Bavel J, Skalky CS, Ghannam AF. Effects of montelukast and beclomethasone on airway function and asthma control. *J Allergy Clin Immunol* 2002;**110**:847-54.
5. Nayak AS, Phillip G, Lu S, Malice M-P, Reiss TF. Efficacy and tolerability of montelukast alone or in combination with loratadine in seasonal allergic rhinitis: a multicenter, randomized, double-blind, placebo controlled trial performed in the fall. *Ann Allergy Asthma Immunol* 2002;**88**: 592-600.
6. British Thoracic Society; Scottish Intercollegiate Guidelines Network. British guideline on the management of asthma. *Thorax* 2003;**58**(Suppl 1):1-94.
7. Booth H, Richmond I, Ward C, Gardiner PV, Harkawat R, Walters EH. Effect of high dose inhaled fluticasone propionate on airway inflammation in asthma. *Am J Respir Crit Care Med* 1995;**152**:45-52.
8. Wenzel SE, Szefler SJ, Leung DY, Sloan SI, Rex MD, Martin RJ. Bronchoscopic evaluation of severe asthma. Persistent inflammation associated with high dose glucocorticoids. *Am J Respir Crit Care Med* 2000;**162**:578-85.
9. Price DB, Hernandez D, Magyar P, Fiterman J, Beeh KM, James IG. Randomized controlled trial of montelukast plus inhaled budesonide versus double dose inhaled budesonide in adult patients with asthma. *Thorax* 2003; **58**:211-6.
10. Price DB, Swern A, Tozzi CA, Philip G, Polos P. Effect of montelukast on lung function in asthma patients with allergic rhinitis: analysis from the COMPACT trial. *Allergy* 2006;**61**:737-42.
11. Bjermer L, Bisgaard H, Bousquet J *et al.* Montelukast and fluticasone compared with salmeterol and fluticasone in protecting against asthma exacerbation in adults: one year, double blind, randomised, comparative trial. *BMJ* 2003;**327**:891-6.
12. Currie GP, Lee DK, Haggart K, Bates CE, Lipworth BJ. Effects of montelukast on surrogate inflammatory markers in corticosteroid-treated patients with asthma. *Am J Respir Crit Care Med* 2003;**167**:1232-8.
13. Barnes N, Laviolette M, Allen D *et al.* Effects of montelukast compared to double dose budesonide on airway inflammation and asthma control. *Respir Med* 2007;**101**: 1652-8.
14. American Thoracic Society. Standards for the diagnosis and care of patients with chronic obstructive pulmonary disease and asthma. *Am Rev Respir Dis* 1987;**136**:225-44.
15. Hovarth I, Hunt J, Barnes PJ. Exhaled breath condensate: methodological recommendations and unresolved questions. *Eur Respir J* 2005;**26**:523-48.
16. Matsunaga K, Yanagisawa S, Ichikawa T *et al.* Airway cy-

tokine expression measured by means of protein array in exhaled breath condensate: Correlation with physiologic properties in asthmatic patients. *J Allergy Clin Immunol* 2006;**118**:84-90.
17. Reddel HK, Salome CM, Peat JK, Woolcock AJ. Which index of peak expiratory flow is most useful in the management of stable asthma? *Am J Respir Crit Care Med* 1995; **151**:1320-5.
18. Matsunaga K, Kanda M, Hayata A *et al.* Peak expiratory flow variability adjusted by forced expiratory volume in one second is a good index for airway responsiveness in asthmatics. *Intern Med* 2008;**47**:1107-12.
19. National Heart, Lung, and Blood Institute/World Health Organization. *Global Initiative for Asthma, Global Strategy for Asthma Management and Prevention*, Updated 2006. Bethesda: NIH Publication, 2006.
20. Braunstahl GJ, Kleinjan A, Overbeek SE, McEuen AR, Walls AF. Segmental bronchial provocation induces nasal inflammation in allergic rhinitis patients. *Am J Respir Crit Care Med* 2000;**161**:2051-7.
21. Corren J, Adinoff AD, Irvin CG *et al.* Changes in bronchial responsiveness following nasal provocation with allergen. *J Allergy Clin Immunol* 1992;**89**:611-8.
22. Lee E, Robertson T, Smith J *et al.* Leukotriene receptor and synthesis inhibitors reverse survival in eosinophils of asthmatic individuals. *Am J Respir Crit Care Med* 2000; **161**:1881-6.
23. Kawano T, Matsuse H, Kondo H *et al.* Cysteinyl leukotrienes induce nuclear factor kB activation and RANTES production in a murine model of asthma. *J Allergy Clin Immunol* 2003;**112**:369-74.
24. Rajakulasingam K, Hamid Q, O'Brien F *et al.* RANTES in human allergen-induced rhinitis. *Am J Respir Crit Care Med* 1997;**155**:696-703.
25. Ueda T, Takeno S, Furukido K *et al.* Leukotriene receptor antagonist pranlukast suppresses eosinophil infiltration and cytokine production in human nasal mucosa of perennial allergic rhinitis. *Ann Otol Rhinol Laryngol* 2003;**112**: 955-61.
26. Gaga M, Lambrou P, Papageorgiou N *et al.* Eosinophils are a feature of upper and lower airway pathology in non-atopic asthma, irrespective of the presence of rhinitis. *Clin Exp Allegy* 2000;**30**:663-9.
27. Higashi N, Taniguchi M, Mita H, Ishii T, Akiyama K. Nasal blockage and urinary leukotriene E4 concentration in patients with seasonal allergic rhinitis. *Allergy* 2003;**58**: 476-80.
28. Miadonna A, Tedeschi A, Leggieri E *et al.* Behavior and clinical relevance of histamine and leukotrienes C4 and B4 in grass pollen-induced rhinitis. *Am Rev Respir Dis* 1987;**136**:357-62.
29. Pavord ID, Ward R, Woltmann G *et al.* Induced sputum eicosanoid concentrations in asthma. *Am J Respir Crit Care Med* 1999;**160**:1905-9.
30. Wenzel SE, Larsen GL, Johnston K *et al.* Elevated levels of leukotriene C4 in bronchoalveolar lavage fluid from atopic asthmatics after endobronchial allergen challenge. *Am Rev Respir Dis* 1990;**142**:112-9.
31. Jeffery PK, Haahtela T. Allergic rhinitis and asthma: inflammation in a one-airway condition. *BMC Pulm Med* 2006;**6**(Suppl 1):S5.
32. Chung KF, Barnes PJ. Cytokines in asthma. *Thorax* 1999; **54**:825-57.
33. Gavreau GM, Watson RM, O'Byrne PM *et al.* Kinetics of allergen-induced eosinophilic cytokine production and airway inflammation. *Am J Respir Crit Care Med* 1999; **160**:640-7.
34. Castro M, Bloch SR, Jenkerson MV *et al.* Asthma exacerbations after glucocorticoid withdrawal reflect T cell recruitment to the airway. *Am J Respir Crit Care Med* 2004; **169**:842-9.
35. Gonzalo JA, Lloyd C, Wen D *et al.* The coordinated action of CC chemokines in the lung orchestrates allergic inflammation and airway responsiveness. *J Exp Med* 1998; **188**:157-67.

Respiratory Physiology & Neurobiology 166 (2009) 61–67

Contents lists available at ScienceDirect

Respiratory Physiology & Neurobiology

journal homepage: www.elsevier.com/locate/resphysiol

Regulation of adenosine 5′-triphosphate (ATP)-gated $P2X_4$ receptors on tracheal smooth muscle cells

Miyuki Nagaoka[a], Masayuki Nara[b,*], Tsutomu Tamada[a], Hiroaki Kume[c], Tetsuya Oguma[c], Toshiaki Kikuchi[d], Jamal Zaini[d], Takuya Moriya[e], Masakazu Ichinose[f], Gen Tamura[a], Toshio Hattori[a]

[a] Division of Infectious and Respiratory Diseases, Department of Internal Medicine, Tohoku University School of Medicine, Aoba-ku, Sendai, Japan
[b] Division of Comprehensive Medicine, Department of Internal Medicine, Tohoku University School of Medicine, 1-1 Seiryo-machi, Aoba-ku, Sendai 980-8574, Japan
[c] Division of Respiratory Medicine, Department of Medicine, Nagoya University School of Medicine, Showa-ku, Nagoya, Japan
[d] Division of Respiratory Medicine, Department of Internal Medicine, Tohoku University School of Medicine, Japan
[e] Department of Pathology, Kawasaki Medical University, Kurashiki, Japan
[f] The Third Department of Internal Medicine, Wakayama Medical University, Wakayama, Japan

ARTICLE INFO

Article history:
Accepted 8 February 2009

Keywords:
Purinergic receptor
Airway smooth muscle
Ivermectin

ABSTRACT

We examined the effects of extracellular adenosine 5′-triphosphate (ATP) on single airway smooth muscle (ASM) cells from porcine trachea using a patch-clamp technique. ATP induced a sustained inward current. Phospholipase C inhibitor U-73122 failed to inhibit the current, suggesting the involvement of P2X receptor. A specific effecter of $P2X_4$, ivermectin, augmented the current indicating the existence of $P2X_4$ receptors. Immunohistochemistry and reverse transcription/polymerase chain reaction analysis and Western blot analysis also showed the distribution of the $P2X_4$ receptors. The inward current was reduced by SKF-96365, an inhibitor of both voltage-dependent Ca^{2+} channels (VDCCs) and voltage-independent Ca^{2+} channels, although a VDCC antagonist, verapamil, did not affect the current. SKF-96365 caused complete suppression of both the increase in the intracellular Ca^{2+} concentration and the contraction of ASM cells induced by ATP. Our results demonstrate that $P2X_4$ receptors exist on ASM and that the receptors are responsible for Ca^{2+} influx. These findings suggest that the Ca^{2+} influx regulated by $P2X_4$ receptors plays an important role in ASM contraction by a pathway distinct from VDCC.

1. Introduction

Adenosine 5′-triphosphate (ATP) is an endogenous purine nucleotide which acts as a ubiquitous extracellular messenger binding to purinergic 2 (P2) receptors on the cell surface (Dubyak and el-Moatassim, 1993). P2 receptors are subclassified into P2X and P2Y subtypes on the basis of amino acid sequence homology and distinct signal transduction mechanisms (Abbracchio and Burnstock, 1994; North, 2002). P2X receptors are cation-selective channels gated by extracellular ATP, initiating an influx of extracellular cations into the cell (North, 2002; Khakh and North, 2006). On the other hand, P2Y receptors belong to the superfamily of G-protein-coupled receptors (North, 2002). All cloned and functionally expressed P2Y receptors are able to couple through the inositol 1,4,5-trisphosphate (IP_3) pathway involving the activation of phospholipase C (PLC) (von Kugelgen and Wetter, 2000). P2 receptors have been found on the cell membranes of many different cell types and their stimulation has a wide range of effects (Dubyak and el-Moatassim, 1993). In airway, ATP mediates important effects. Extracellular ATP is generally thought to interact with the parasympathetic limb of the autonomic nervous system resulting in neurogenic bronchoconstriction and neurogenic inflammation, and to modulate the function of various immune cells including mast cells, eosinophils, and dendritic cells, which in turn induce hypersensitivity responses (Pelleg and Schulman, 2002). ATP is also a potent stimulator of airway surface fluid secretion through the stimulation of submucosal glands, and epithelial and goblet cells (Lethem et al., 1993; Shimura et al., 1994). Although the effects of extracellular ATP on the airway have been investigated extensively, the direct effect of ATP on airway smooth muscle (ASM) cells has not been well characterized. Especially, information about the ionic mechanisms of ASM in response to ATP is controversial. Bergner and Sanderson (2002) reported that ATP induced a transient contraction and cytosolic Ca^{2+} oscillation mediated by P2Y purinoceptors in mouse lung. On the other hand, in rat airways, ATP induced a transient contractile response due to extracellular Ca^{2+} influx. The extracellular Ca^{2+} influx occurs through voltage-dependent Ca^{2+} channels (VDCCs) activated by external Na^+ entry through P2X receptors (Mounkaïla et al., 2005).

* Corresponding author. Tel.: +81 22 717 7587; fax: +81 22 717 7508.
E-mail address: mnara@mail.tains.tohoku.ac.jp (M. Nara).

1569-9048/$ – see front matter © 2009 Elsevier B.V. All rights reserved.
doi:10.1016/j.resp.2009.02.002

It has been established that the smooth muscle contraction is regulated by the intracellular Ca^{2+} concentration ($[Ca^{2+}]i$) (Somlyo and Somlyo, 1994). An increase in $[Ca^{2+}]i$ by agonists plays an important role in the contraction of airway smooth muscle (Gerthoffer, 1991; Ito et al., 2001). Reports demonstrated that the contraction induced by receptor agonists is insensitive to inhibitors of voltage-dependent Ca^{2+} channels in ASM, indicating that Ca^{2+} influx other than from VDCC may be involved in contraction by agonists (Benham and Tsien, 1987; Murray et al., 1993; Gorenne et al., 1998; Ito et al., 2002). To date, however, little is known about the Ca^{2+} influx pathway responsible for the contraction of ASM by ATP.

In this study, we investigated the effect of extracellular ATP on single ASM cells from porcine trachea. The aims of this study were to determine the purinergic receptor subtype on the ASM and to clarify the relationship between the receptor and the intracellular Ca^{2+} mobilization responsible for the contraction of ASM.

2. Materials and methods

2.1. Cell dissociation

ASM cells were dissociated from porcine tracheae obtained from a local abattoir. The smooth muscle layer was isolated from the posterior membranous portion of the trachea by removing surrounding connective tissue and epithelium, and the isolated smooth muscle strips were cut into small pieces. Then, these smooth muscle pieces were dispersed enzymatically into single cells with collagenase (0.125 mg/ml), papain (1 mg/ml), and DL-dithiothreitol (2 mM) for 40 min at 37 °C. After incubation, the tissue pieces were gently agitated, and single smooth muscle cells were resuspended in the extracellular solution. The individual smooth muscle cells were relaxed and spindle-shaped.

2.2. Electrophysiology

A standard patch-clamp recording technique was used as previously described (Nara et al., 1998; Oshiro et al., 2000). Briefly, an EPC9 (HEKA Electronics, Dramstadt, Germany) patch-clamp amplifier was used to measure ionic currents. Currents were low-pass filtered at 1 kHz and monitored on both a built-in software oscilloscope and a thermal pen recorder (RECTI-HORITZ-8K; Nippondenki Sanei, Tokyo, Japan) with a bandwidth of 0–300 Hz. The patch electrodes (Drummond Scientific Co., Broomall, PA) had a tip resistance of 2–5 MΩ. The junction potential between the patch-pipette and bath solution was nulled by the amplifier circuitry. After establishing a high-resistance (>2 GΩ) tight seal, the whole-cell configuration was obtained by rupturing the patch membrane with negative pressure applied to the pipette tip. The capacitance current and series resistance were compensated using the amplifier circuitry. The access resistance was always less than 40 MΩ, and 75–80% series resistance compensation was employed. The solutions used were of the following composition (in mM): extracellular (bath) solution, 140 NaCl, 4.7 KCl, 1.13 $MgCl_2$, 1.2 $CaCl_2$, 10 glucose, and 10 Hepes; and intracellular (pipette) solution, 140 KCl, 1.13 $MgCl_2$, 10 glucose, 10 Hepes, 5 ethyl glycol-*bis*(β-aminoethyl ether)-*N,N,N′,N′*-tetraacetic acid (EGTA), 1.72 $CaCl_2$, and 1 Na_2-ATP, adjusted to pH 7.2 with NaOH (bath solution) or KOH (pipette solution). The free Ca^{2+} in the pipette solution was 100 nM (Fabiato, 1988). All experiments were carried out at room temperature, 22–24 °C. The fluids were superfused over the cell by hydrostatic pressure-driven application (40–50 cm H_2O) through polyethylene tubes (0.5 mm inner diameter). The morphology of the smooth muscle cells did not change even after employment of the whole-cell configuration. In these studies, only those cells that contracted in response to ATP were used.

2.3. Immunohistochemical studies

Specimens of porcine trachea were fixed in periodate–lysine–paraformaldehyde at 4 °C for 24 h. After washing in sucrose (10%, 15%, and 20%)/phosphate-buffered saline (PBS) for 2 h each, they were embedded in OCT compound in liquid nitrogen and stored at −80 C until use. The staining was performed with the polymer immune complex method. Technical details concerning the procedures are described by Tamada et al. (2000). Cryostat sections (5 μm) were stained for the rat $P2X_4$ purinergic receptor using monoclonal rabbit anti-rat $P2X_4$ receptor antibody specific to a 370–388 amino acid residue. Slides were incubated with the primary antibody diluted 50-fold in Tris-buffered saline (0.05 M Tris and 0.15 M NaCl, pH 7.6) with 2% NaCl to increase the specificity of antigen–antibody interactions (Yeung et al., 2004). After overnight incubation at 4 °C, the slides were incubated with 10% normal goat serum containing PBS and peroxidase blocking reagent to block the endogenous peroxidases. Secondary, slides were incubated with anti-rabbit Ig goat polyclonal Igs binding with peroxidase-labeled dextran for 30 min at room temperature. Slides were then developed by exposure to diaminobenzidine (DAB) for substrate for 5 min at room temperature according to the manufacturer's protocol, and counterstained with hematoxylin.

2.4. Western blot analysis of $P2X_4$ receptor expression

1 g of porcine tissue (tracheal smooth muscle, tongue, heart, diaphragm) was homogenized in 5 ml ice-cold RIPA buffer, and centrifuged at 15,000 × *g* for 30 min at 4 °C. The proteins were separated on SDS-polyacrylamide gels and electroblotted onto PVDF membrane. The blots were incubated with a blocking solution containing 5% (v/v) nonfat milk overnight at 4 °C and then with rabbit polyclonal anti-$P2X_4$ purinergic receptor at 1:200 in BT PBS (0.05% Tween-20, 1% BSA in PBS) for 1 h at 37 °C. Following washes with PBST, the membranes were incubated with horseradish peroxidase secondary anti rabbit IgG for 1 h at 37 °C (1:5000) and visualized on film using an ECL kit. To compare protein loading, the blots were probed with affinity purified anti-actin antibody. The $P2X_4$ receptor is known to exist as glycosylated (65 kDa) and nonglycosylated (46 kDa) protein (Gonzales et al., 2007).

2.5. Reverse transcription/polymerase chain reaction (RT-PCR) analysis of $P2X_4$ receptor messenger RNA

Freshly isolated porcine tracheae were frozen and stored until the experiments to analyze the expression of $P2X_4$ receptor mRNA. Total RNA was extracted from tracheal smooth muscle cells isolated by capture microdissection (Takara Bio Inc., Shiga, Japan) and was converted to cDNA according to the manufacturer's instructions. Since porcine $P2X_4$ receptor gene sequences were not found in any databases, we referred to the human, mice and rat $P2X_4$ receptor gene sequences and prospected the porcine $P2X_4$ receptor gene sequence so that its product could have high homologies (Takara Bio Inc., Shiga, Japan). As a positive control PCR product, we selected a porcine β-actin gene sequence from the NCBI database. Oligonucleotide primers used in PCR for $P2X_4$ receptor were 5′-CAGGACATGGCCGTCGAGGGA-3′ and 5′-CTCCGGCTTGGCGCTCTAGG-3′ and amplified 311 bp of the $P2X_4$ receptor cDNA segment. Primers for β-actin were 5′-TCGTCACCAACTGGGACGC-3′ and 5′-GACTACCTC-ATGAAGATCCTGACG-5′ and amplified 359 bp of the β-actin

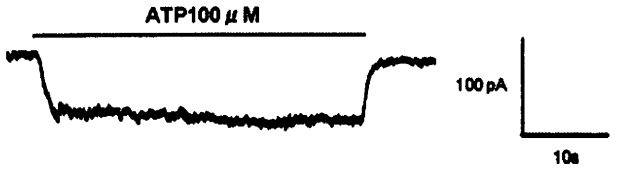

Fig. 1. Effect of ATP on airway smooth muscle cells. (A) A representative trace of ATP (100 μM)-induced inward current. The activation of the inward current was maintained in the continuous presence of ATP. The membrane potential (Mp) was held at −40 mV.

cDNA segment. The thermal cycling conditions were as follows: first, denaturation at 94 °C for 5 min, 35 cycles of denaturation at 94 °C for 30 s, annealing at 55 °C for 30 s and extension at 72 °C for 30 s, and finally extension at 72 °C for 4 min. The reaction products were run on a 1.5% agarose gel and visualized after electrophoresis by ethidium bromide staining.

2.6. Isometric force records and measurement of fura-2 fluorescence

The methods are essentially similar to those described previously (Kume et al., 2001; Ito et al., 2002; Oguma et al., 2007). The smooth muscle layer was isolated from the posterior membranous portion of the porcine trachea by removing the surrounding connective tissue and epithelium. Muscle strips 2 mm long by 1 mm wide were prepared for isometric force recording and $[Ca^{2+}]i$ measurements. The muscle strips were placed horizontally in the chamber, and then were treated with 10 μM acetoxymethyl ester of fura-2 (fura-2/AM) for 4 h at room temperature (22–24 °C). The noncytotoxic detergent pluronic F-127 (0.01%wt/vol.) was added to increase the solubility of fura-2/AM. After loading, the chamber was perfused with normal bathing solution at 37 °C for 50 min to wash out the extracellular fura-2/AM. The normal bathing solution was composed of (in mM): 137 NaCl, 5.9 $KHCO_3$, 2.4 $CaCl_2$, 1.2 Mg Cl_2, and 11.8 glucose, bubbled with a mixture of 99% O_2 and 1% CO_2 (pH 7.4). The bathing solution was infused into the organ bath at a constant flow of 3 ml/min. The isometric force and fura-2 fluorescence of muscle strips were measured simultaneously using a displacement transducer and a spectrofluorometer (CAF-110; Japan Spectoscopic, Tokyo, Japan). The intensities of fluorescence due to excitation at 340 (F_{340}) and 380 (F_{380}) nm were measured after background subtraction. The absolute amount of $[Ca^{2+}]i$ was not calculated because the dissociation constant of fura-2 for Ca^{2+} in smooth muscle may be different from that observed in vitro. Therefore, the ratio of F_{340} to F_{380} (F_{340}/F_{380}) was used as a relative indicator of $[Ca^{2+}]i$. Measurements of the tension and F_{340}/F_{380} were made when the response to methacholine (MCh) had attained a steady state. The temperature of the organ bath was maintained at 37 °C.

2.7. Chemicals

Hepes and Fura-2 were purchased from Dojin Co, Ltd., Kumamoto, Japan. Collagenase was from Wako Pure Chemicals, Osaka, Japan. U-73122 was purchased from Carbiochem Co., La Jolla, CA. OCT compound was from Miles Laboratories, Naperville, IL. Peroxidase blocking regent, peroxidase-labeled dextran, and diaminobenzidine were from Dako Co., Carpinteria, CA. Monoclonal rabbit anti human $P2X_4$ receptor antibody was purchased from Alomone Labs Inc., Jerusalem, Israel. The ECL kit was from Amersham Pharmacica Biotec Co. Other chemicals including ATP were all purchased from Sigma Chemical Co., St. Louis, MO.

2.8. Statistical analysis

All data are shown as means ± standard error of the mean. For mean comparison, the two-tailed paired or unpaired Student's *t*-test was used. A value of $P < 0.05$ was considered statistically significant. *n* denotes the number of experiments in different cells.

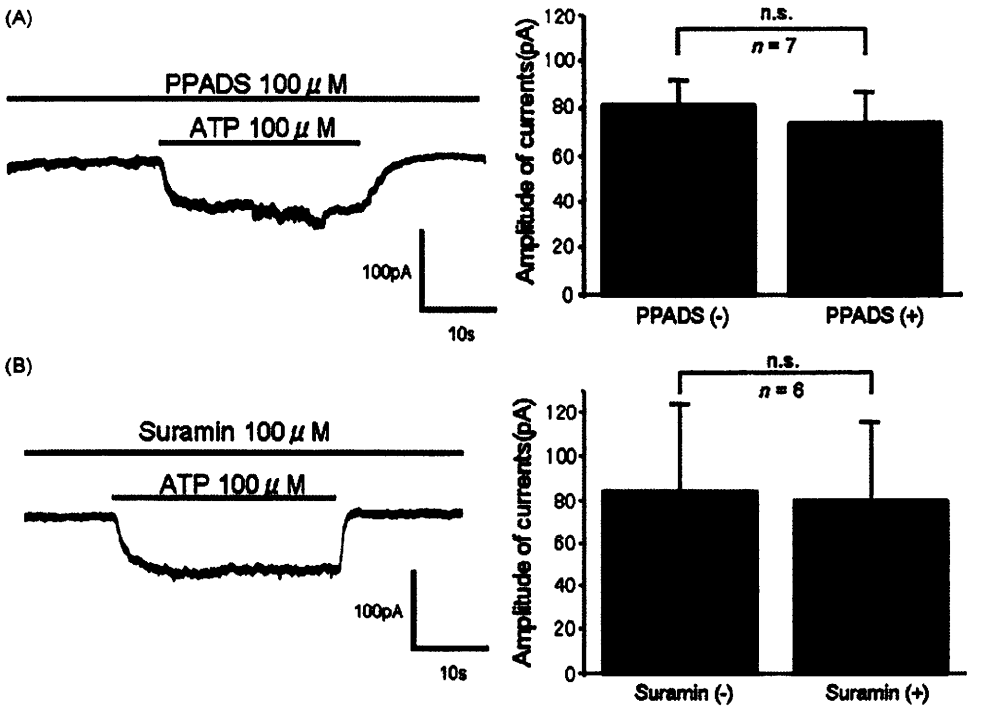

Fig. 2. Effects of PPADS and suramin on ATP-evoked current. Both 100 μM PPADS (A) and 100 μM suramin (B) failed to inhibit the ATP-evoked inward current. The holding potential was −40 mV. n.s., not significant.

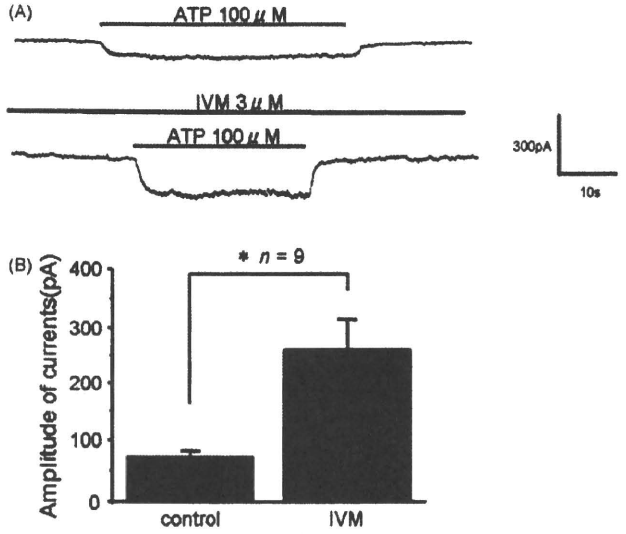

Fig. 3. Effect of ivermectin (IVM) on ATP-evoked current. (A) Representative records of 100 μM ATP-evoked current before (*upper*) and after (*lower*) the addition of IVM (3 μM). IVM potentiates the amplitude of the ATP-evoked current. The holding potential was −40 mV. (B) Summary of data from 9 cells showing that IVM potentiates ATP-evoked currents. The amplitude of the currents increased by 360% in the presence of IVM. * represents $P < 0.01$.

3. Results

3.1. Electrophysiological effects of ATP on ASM

Fig. 1 shows the membrane currents recorded in the whole-cell configuration of the patch-clamp technique in response to 100 μM extracellular ATP at a holding potential of −40 mV. ATP elicited an inward current. The current amplitudes were 78.8 ± 26.6 pA ($n = 17$ cells from 10 animals). The activation of the inward current was maintained in the continuous presence of ATP. ATP was then washed away and the current returned to its base line within a few seconds.

3.2. $P2X_4$ receptor-mediated currents

We first used the PLC inhibitor U-73122 in order to examine whether the P2Y signaling pathway is involved because ATP-mediated activation of P2Y receptors has been shown to activate PLC with the subsequent generation of IP_3 (von Kugelgen and Wetter, 2000). Exposure of ASM to U-73122 (10 μM) for 30 min did not alter the induction of the inward current by ATP (74.2 ± 17.4 pA for ATP alone and 70.8 ± 30.1 pA for ATP in the presence of U-73122; $P = 0.83$; $n = 6$ cells from 4 animals), suggesting that not P2Y receptors but P2X receptors are involved in the ATP-induced current. We then applied the P2X receptor antagonists PPADS and suramin. As shown in Fig. 2, however, these antagonists failed to inhibit the current (81.4 ± 27.2 pA for ATP alone and 73.8 ± 33.1 pA for ATP plus PPADS; $P = 0.30$; $n = 7$ cells from 3 animals, 84.2 ± 40.0 pA for ATP alone and 80.0 ± 36.0 pA for ATP plus suramin; $P = 0.38$; $n = 6$ cells from 5 animals, respectively). As far as P2X receptors are

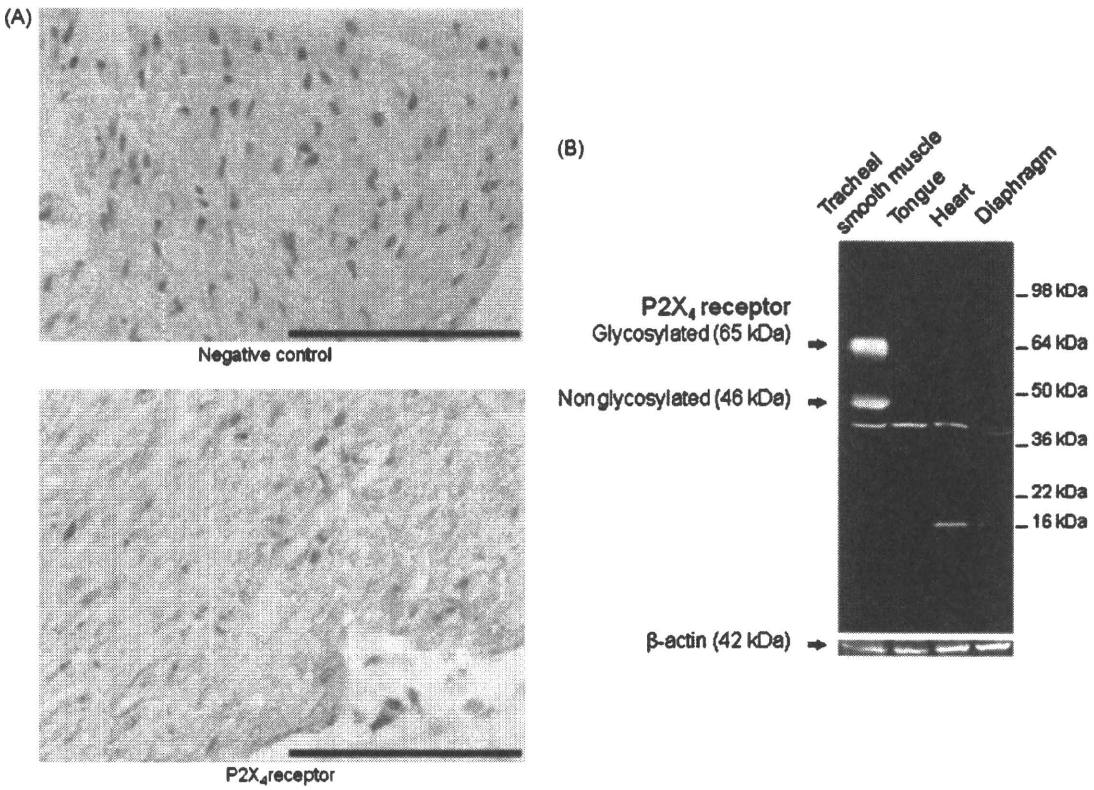

Fig. 4. (A) Immunolocalization of the $P2X_4$ receptor in porcine ASM. Polymer immune complex stain of porcine airway smooth muscles using rabbit mAb against human $P2X_4$-R. The section was with mAb against $P2X_4$-R, and was counterstained weakly with hematoxylin. The positive brown stain was detected in smooth muscle cells. No significant label was detected in porcine airway smooth muscle cells in the case of negative control Igs (*bar*: 100 μm). (B) $P2X_4$ receptor expression in ASM by Western blot analysis. The abundance of $P2X_4$ receptor protein (65/46 kDa) in the porcine tracheal smooth muscle was determined. Controls included extracts prepared from porcine tongue, heart, and diaphragm. Expression of β-actin is shown as a marker for protein loading.

concerned, most of the antagonists available are highly limited in terms of receptor-affinity, subtype-selectivity (Lambrecht, 2000). PPADS and suramin are known to be ineffective as antagonists to $P2X_4$ receptors although they are specific for other P2X receptors (Soto et al., 1996; Khakh et al., 1999; Khakh and North, 2006). Then, we applied ivermectin (IVM), a specific positive allosteric effecter of $P2X_4$ (Khakh et al., 1999; Priel and Silberberg, 2004; Silberberg et al., 2007), to ASM cells. As shown in Fig. 3A, in the presence of 3 μM IVM in the extracellular solution, the current in response to ATP increased. IVM significantly increased the current by 360% (72.2 ± 10.6 pA for ATP alone and 261.1 ± 53.8 pA for ATP plus IVM; $P < 0.01$; $n = 9$ cells from 4 animals) (Fig. 3B). We also employed immunohistochemistry to confirm the presence of $P2X_4$ receptors, supporting the identification of the receptors carried out by pharmacological methods as described above. As shown in Fig. 4A, immunofluorescence for $P2X_4$ receptors was evident in ASM cells. $P2X_4$ receptor expression was also confirmed by Western blot analysis (Fig. 4B). In addition, the $P2X_4$ expression of the smooth muscles was demonstrated by RT-PCR (Fig. 5). The intactness of RNA was confirmed by amplification of β-actin.

3.3. Ca^{2+} entry through the ATP-activated inward current

It is known that ATP acting through P2X purinoceptors can activate a cation current permeant to Ca^{2+} ions in several types of cells (Benham, 1989; Nakazawa et al., 1991; Evans et al., 1996; Capiod, 1998; Lundy et al., 2002). A recent report suggested that the extra cellular Ca^{2+} influx occurred through VDCC activated by external Na^+ entry through P2X receptors (Mounkaïla et al., 2005). In the first instance, we applied SKF-96365, an inhibitor of both VDCC and voltage-independent Ca^{2+} channel (VICC) (Merrit et al., 1990), to ASM cells. Fig. 6A shows the effect of SKF-96365 on the inward current evoked by ATP. The current was reduced by 47% in the presence of 100 μM SKF-96365 (78.3 ± 7.5 pA for ATP alone and 41.7 ± 7.9 pA for ATP in the presence of 100 μM SKF-96365; $P < 0.01$; $n = 9$ cells from 5 animals) (Fig. 6B). On the other hand, the current was unaffected by the VDCC antagonist verapamil ($n = 5$ cells from 4 animals) (Fig. 6C), suggesting that VDCC is not involved in the current. These data indicate that the ATP-induced inward current involves the influx of Ca^{2+}, and that the Ca^{2+} influx in response to ATP is mediated not by VDCC but by the $P2X_4$ receptor.

Fig. 5. cDNA segments of $P2X_4$ receptor (left panel) and β-actin (right panel) amplified by RT-PCR from porcine trachea. Tracheal smooth muscle cells selectively extracted from porcine tracheae by laser capture microdissection showed a clear band of $P2X_4$ receptor cDNA. The 311 bp and 359 bp DNA segments were expected to be amplified from the $P2X_4$ receptor cDNA and β-actin cDNA, respectively.

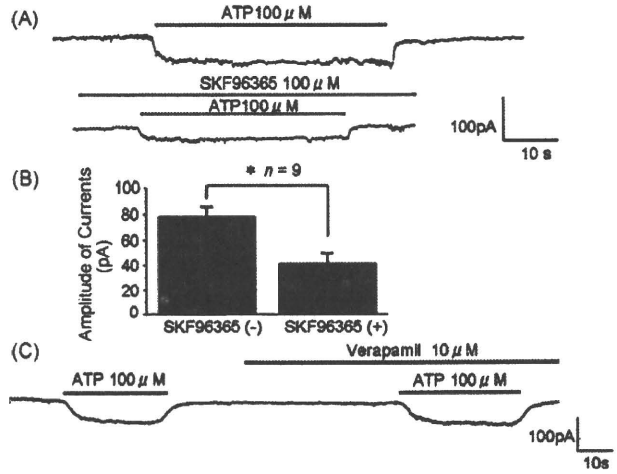

Fig. 6. Effect of SKF-96365 and verapamil on ATP-evoked current. (A) Representative records of 100 μM ATP-evoked current before (*upper*) and after the addition (*lower*) of SKF-96365 (100 μM). SKF-96365 reduced the ATP-evoked current. The holding potential was −40 mV. (B) Summary of data from 9 cells showing that SKF-96365 significantly reduced the ATP-evoked currents. The amplitude of the currents reduced by 47% in the presence of SKF-96365. * represents $P < 0.01$. (C) A representative trace of 100 μM ATP-evoked current before and after the addition of verapamil. Verapamil did not affect the current.

3.4. Effect of SKF-96365 on contraction and Ca^{2+} mobilization induced by ATP

We examined the extent to which Ca^{2+} activated by ATP would contribute to the contraction using fura-2 fluorescence methods and by measuring the isometric force. As shown in Fig. 7A, the application of 100 μM ATP caused tonic contraction and a rapid increase in F_{340}/F_{380}. The increase in F_{340}/F_{380} was sustained without a transient increase in the continuous presence of ATP. When the tension and F_{340}/F_{380} in response to 1 μM methacholine were taken as 100%, these values by 100 μM ATP were 86.8 ± 6.6, and 90.6 ± 4.8%, respectively ($n = 6$). When 100 μM SKF-96365 was applied to the tissue pre-contracted by 100 μM ATP, SKF-96365 caused roughly a complete suppression of both the tension and the increase in F_{340}/F_{380} induced by ATP. As shown in Fig. 7B, the application of SKF-96365 resulted in a concentration-dependent inhibition of the tension and F_{340}/F_{380} induced by 100 μM ATP. When 10 μM SKF-96365 was applied in the same way, the values of percent contraction and percent F_{340}/F_{380} were 65.1 ± 9.8, and 72.8 ± 12.1%, respectively ($n = 6$). When the concentration of SKF-96365 was increased to 100 μM, those values were decreased to 3.8 ± 4.0, and 2.1 ± 1.6%, respectively ($n = 6$). Together with the effect of SKF-96365 on the inward current (Fig. 6), these data suggest that a significant portion of the inward current following $P2X_4$ receptor activation, that is Ca^{2+} influx, contributes to the smooth muscle contraction.

4. Discussion

The present study provides evidence for an ATP-induced inward current after stimulation of $P2X_4$ receptors in porcine ASM cells. It further demonstrates the physiological relevance of this current to Ca^{2+} mobilization in these cells.

Purinoceptors are a diverse group of purine- and pyrimidine-sensitive receptors that have been divided into two major families, classified as P2X and P2Y (Dubyak and el-Moatassim, 1993). P2X receptors are ligand-gated, cation-selective channels, whereas P2Y receptors are G-protein-coupled receptors (North, 2002). All cloned and functionally expressed P2Y receptors are able to couple through

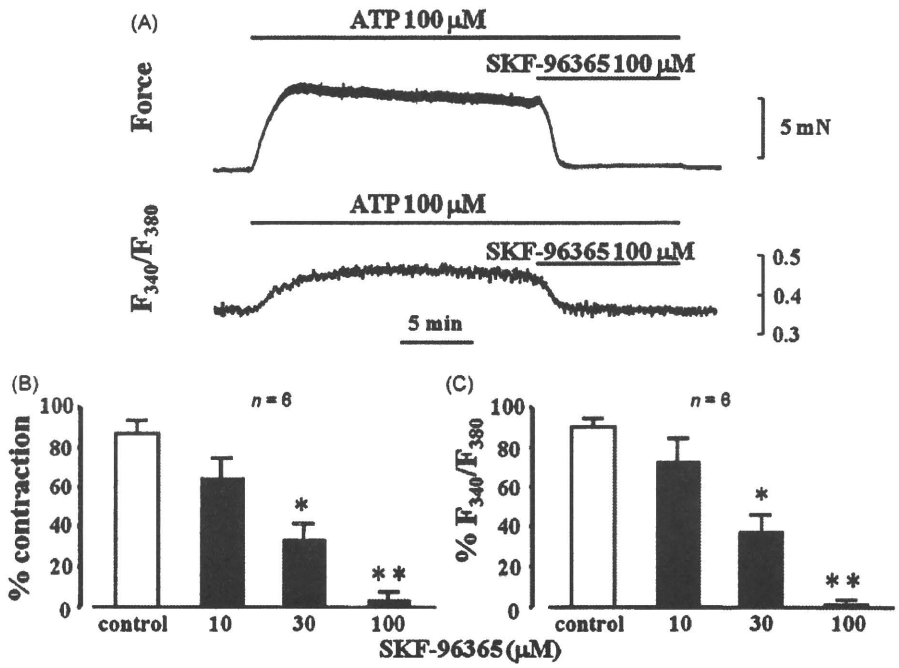

Fig. 7. Effects of SKF-96365 on the contraction and Ca^{2+} mobilization induced by ATP. (A) A representative trace showing the effects of SKF-96365 on the change in force (upper trace) and F_{340}/F_{380} (lower trace). (B) The values of percent contraction and percent F_{340}/F_{380} for 100 μM ATP with SKF-96365 (10–100 μM) inhibition. * and ** represent $P < 0.05$ and $P < 0.01$, respectively.

the IP_3 pathway involving the activation of PLC (von Kugelgen and Wetter, 2000). Our data indicate that the ATP-activated inward current is associated with P2X receptors because U-73122, a PLC inhibitor, failed to inhibit the current. To date, seven clones of P2X receptors expressed in various cells have been identified. These P2X receptors show differences in their sensitivity to antagonists and in their kinetics of desensitization (Evans and Surprenant, 1996; North, 2002). In the present study, the ATP-induced current showed little desensitization (Fig. 1) and, moreover, this current was not blocked by the conventional antagonists of P2X receptors, PPADS and suramin (Fig. 2). Among the P2X receptors, the $P2X_4$ receptor is unusual in its insensitivity to blockade by these antagonists (Soto et al., 1996; North, 2002). ATP-induced current through $P2X_4$ receptors is also reported to show non-desensitization (Evans and Surprenant, 1996). In addition, the most useful distinguishing feature of ATP-evoked currents by $P2X_4$ receptors is their potentiation by IVM (Khakh et al., 1999; Priel and Silberberg, 2004; Silberberg et al., 2007). IVM is a specific allosteric effector of $P2X_4$. It can increase the gating of the $P2X_4$ channel. The $P2X_4$ channel is sensitive to IVM, whereas other subtypes of P2X receptor are insensive to the compound (Khakh et al., 1999; Jelínkova et al., 2008). Collectively, our observations clearly indicate the functional expression of $P2X_4$ receptors on ASM cells. The existence of the receptors was also evident by immunostaining, RT-PCR and Western blot analysis (Figs. 4 and 5). However, as we do not have a specific $P2X_4$ receptor antagonist, further investigation may be required to confirm absolutely the function of the $P2X_4$ receptor.

It has been established that the smooth muscle contraction is regulated by $[Ca^{2+}]_i$ (Somlyo and Somlyo, 1994). An increase in $[Ca^{2+}]_i$ by agonists plays an important role in the contraction of airway smooth muscle (Gerthoffer, 1991; Ito et al., 2001). It is generally accepted that voltage-dependent Ca^{2+} channels and voltage-independent Ca^{2+} channels (VICCs), which include a receptor-operated Ca^{2+} permeable channel, a store-operated Ca^{2+} channel and a transmitter-gated cation channel, are involved in Ca^{2+} influx and the induced contraction (Worley and Kotlikoff, 1990; Large, 2002; Egan and Khakh, 2004). P2X receptors are known as transmitter (ATP)-gated cation channels (Egan and Khakh, 2004; Abbracchio and Burnstock, 1994; North, 2002). Fig. 6 shows that a significant proportion (47%) of the inward current following $P2X_4$ receptor activation in physiological solution is carried by calcium. P2X receptors are reported to have a relatively high calcium permeability in several types of cells including smooth muscle cells (Benham, 1989; Evans et al., 1996; Capiod, 1998; Lundy et al., 2002). Several laboratories have quantified Ca^{2+} movement through the pores of P2X channels (Abbracchio and Burnstock, 1994; Egan and Khakh, 2004). For example, Egan and Khakh (2004) estimated that the Ca^{2+} flux ranged from ~3% to 15% of the total current through recombinant $P2X_2$ receptors. Rogers and Dani (1995) have shown that 6.5% of the total charge is carried by Ca^{2+} through the P2X receptor in sympathetic neurons. These studies used different cells, different P2X receptors, and different extracellular and intracellular concentrations of ions. Therefore, it is not possible to directly compare the values among such studies. We estimated the Ca^{2+} flux roughly by using SKF-96365. It is possible that SKF-96365 inhibits cations other than Ca^{2+} (Zhang and Hancox, 2003). Thus, we may have overestimated the Ca^{2+} influx through $P2X_4$ receptors in ASM. However, Figs. 6 and 7 support the role of this inward current in producing airway contraction that is dependent on Ca^{2+} influx. The inward current was resistant to the VDCC antagonist verapamil (Fig. 6). Mounkaïla et al. described that ATP induced a contractile response due to extracellular Ca^{2+} influx and that the extracellular Ca^{2+} influx occurs through VDCC activated by external Na^+ entry through P2X receptors. In our study, however, the contribution of external Na^+ was small because verapamil, a VDCC antagonist, did not work (Fig. 6). Direct Ca^{2+} entry through $P2X_4$ receptors caused the contractile response in our study. The difference between the observations by Mounkaïla et al. and our seems to depend on the species or P2X subtypes. In our study (Fig. 7), ATP elicited a sustained increase in F_{340}/F_{380}, that is $[Ca^{2+}]_i$, without a transient increase. P2Y receptors are known to couple to G-protein and PLC to raise free Ca^{2+} transiently (Ralevic and Burnstock, 1998;

von Kugelgen and Wetter, 2000). Therefore, this lack of a transient increase in $[Ca^{2+}]_i$ together with the effect of U-73122 suggests that P2Y receptors were not involved in this Ca^{2+} mobilization.

ATP is known to be released from storage compartments in nerve terminals, chromaffin cells, circulating platelets, and mast cells (Dubyak and el-Moatassim, 1993; Pelleg and Schulman, 2002). Mast cells stimulated with antigen release not only inflammatory mediators such as histamine but also ATP, which acts as a cell-to-cell messenger, triggering the degranulation of neighbouring mast cells (Osipchuk and Cahalan, 1992). Our results suggest that, in addition to its effect on mast cells, ATP directly affects ASM cell contractility through $P2X_4$ receptors. Considering these results, ATP may also have a direct role in bronchial asthma via its direct action on ASM cells.

5. Conclusion

In conclusion, our study demonstrates that P2X receptors exist on ASM cells, and the evidence presented here suggests that these receptors are of the $P2X_4$ subtype. $P2X_4$ receptors play an important role in Ca^{2+}-dependent events, that is contraction, by a pathway distinct from VDCC.

Acknowledgement

We thank Mr. B. Bell for reading the manuscript.

References

Abbracchio, M.P., Burnstock, G., 1994. Purinoceptors: are there families of P2X and P2Y purinoceptors? Pharmacol. Ther. 64, 445–475.
Benham, C.D., 1989. ATP-activated channels gate calcium entry in single smooth muscle cells dissociated from rabbit ear artery. J. Physiol. 419, 689–701.
Benham, C.D., Tsien, R.W., 1987. A novel receptor-operated Ca^{2+}-permeable channel activated by ATP in smooth muscle. Nature 328, 275–278.
Bergner, A., Sanderson, M.J., 2002. ATP stimulates Ca^{2+} oscillations and contraction in airway smooth muscle cells of mouse lung slices. Am. J. Physiol. Lung Cell. Mol. Physiol. 283, L1271–L1279.
Capiod, T., 1998. ATP-activated cation currents in single guinea-pig hepatocytes. J. Physiol. 507, 795–805.
Dubyak, G.R., el-Moatassim, C., 1993. Signal transduction via P2-purinergic receptors for extracellular ATP and other nucleotides. Am. J. Physiol. Cell Physiol. 265, C577–C606.
Egan, T.M., Khakh, B.S., 2004. Contribution of calcium ions to P2X channel responses. J. Neurosci. 24, 3413–3420.
Evans, R.J., Lewis, C., Virginio, C., Lundstrom, K., Buell, G., Surprenant, A., North, R.A., 1996. Ionic permeability of, and divalent cation effects on, two ATP-gated cation channels (P2X receptors) expressed in mammalian cells. J. Physiol. 497, 413–422.
Evans, R.J., Surprenant, A., 1996. P2X receptors in autonomic and sensory neurons. Semin. Neurosci. 8, 217–223.
Fabiato, A., 1988. Computer programs for calculating total from specified free or free from specified total ionic concentrations in aqueous solutions containing multiple metals and ligands. Methods Enzymol. 157, 378–417.
Gerthoffer, W.T., 1991. Regulation of the contractile element of airway smooth muscle. Am. J. Physiol. Lung Cell. Mol. Physiol. 261, L15–L28.
Gonzales, E., Prigent, S., About-Lovergne, A., Boucherie, S., Tordjmann, T., Jacquemin, E., Combettes, L., 2007. Rat hepatocytes express functional P2X receptors. FEBS Lett. 581, 3260–3266.
Gorenne, I., Labat, C., Gascard, J.P., Norel, X., Nashashibi, N., Brink, C., 1998. Leukotriene D_4 contractions in human airways are blocked by SK&F 96365, an inhibitor of receptor-mediated calcium entry. J. Pharmacol. Exp. Ther. 284, 549–552.
Ito, S., Kume, H., Honjo, H., Katoh, H., Kodama, I., Yamaki, K., Hayashi, H., 2001. Possible involvement of Rho kinase in Ca^{2+} sensitization and mobilization by MCh in tracheal smooth muscle. Am. J. Physiol. Lung Cell. Mol. Physiol. 280, L1218–L1224.
Ito, S., Kume, H., Yamaki, K., Katoh, H., Honjo, H., Kodama, I., Hayashi, H., 2002. Regulation of capacitative and noncapacitative receptor-operated Ca^{2+} entry by Rho-kinase in tracheal smooth muscle. Am. J. Respir. Cell Mol. Biol. 26, 491–498.
Jelínkova, I., Vávra, V., Jindrichova, M., Obsil, T., Zemkova, H.W., Zemkova, H., Stojilkovic, S.S., 2008. Identification of $P2X_4$ receptor transmembrane residues contributing to channel gating and interaction with ivermectin. Pflügers Arch. 456, 939–950.
Khakh, B.S., North, A., 2006. P2X receptors as cell-surface ATP sensor in health and disease. Nature 442, 527–532.
Khakh, B.S., Proctor, W.R., Dunwiddie, T.V., Labarca, C., Lester, H.A., 1999. Allosteric control of gating and kinetics at $P2X_4$ receptor channels. J. Neurosci. 19, 7289–7299.
Kume, H., Ito, S., Ito, Y., Yamaki, K., 2001. Role of lysophosphatidylcholine in the desensitization of β-adrenergic receptors by Ca^{2+} sensitization in tracheal smooth muscle. Am. J. Respir. Cell Mol. Biol. 25, 291–298.
Lambrecht, G., 2000. Agonists and antagonists acting at P2X receptors: selectivity profiles and functional implications. Naunyn Schmiedebergs Arch. Pharmacol. 362, 340–350.
Large, W.A., 2002. Receptor-operated Ca^{2+}-permeable nonselective cation channels in vascular smooth muscle: a physiologic perspective. J. Cardiovasc. Electrophysiol. 13, 493–501.
Lethem, M.I., Dowell, M.L., Scott, M.V., Yankaskas, J.R., Egan, T., Boucher, R.C., Davis, C.W., 1993. Nucleotide regulation of goblet cells in human airway epithelial explants: normal exocytosis in cystic fibrosis. Am. J. Respir. Cell Mol. Biol. 9, 315–322.
Lundy, P.M., Hamilton, M.G., Mei, L., Gong, W., Vair, C., Sawyer, T.W., Frew, R., 2002. Stimulation of Ca^{2+} influx through ATP receptors on rat brain synaptosomes: identification of functional $P2X_7$ receptor subtypes. Br. J. Pharmacol. 135, 1616–1626.
Merrit, J.E., Armstrong, W.P., Benham, C.D., Hallam, T.J., Jacob, R., Jaxa-Chamiec, A., Leigh, B.K., McCarthy, S.A., Moores, K.E., Rink, T.J., 1990. SK&F 96365, novel inhibitor of receptor-mediated calcium entry. Biochem. J. 271, 515–528.
Mounkaïla, B., Marthan, R., Roux, E., 2005. Biphasic effect of extra cellular ATP on human and rat airways is due to multiple P2 purinoceptor activation. Respir. Res. 6, 143–158.
Murray, R.K., Fleischmann, B.K., Kotlikoff, M.I., 1993. Receptor-activated Ca influx in human airway smooth muscle: use of Ca imaging and perforated patch-clamp techniques. Am. J. Physiol. Cell Physiol. 264, C485–C490.
Nakazawa, K., Fujimori, K., Tanaka, A., Inoue, K., 1991. Comparison of adenosine triphosphate- and nicotine-activated inward currents in rat phaeochromocytoma cells. J. Physiol. 434, 647–660.
Nara, M., Sasaki, T., Shimura, S., Oshiro, T., Irokawa, T., Kakuta, Y., Shirato, K., 1998. Effects of histamine and endothelin-1 on membrane potentials and ion currents in bovine tracheal smooth-muscle cells. Am. J. Respir. Cell Mol. Biol. 19, 805–811.
North, R.A., 2002. Molecular physiology of P2X receptors. Physiol. Rev. 82, 1013–1067.
Oguma, T., Ito, S., Kondo, M., Makino, Y., Shimokata, K., Honjo, H., Kamiya, K., Kume, H., 2007. Roles of P2X receptors and Ca^{2+} sensitization in extracellular adenosine triphosphate-induced hyperresponsiveness in airway smooth muscle. Clin. Exp. Allergy 37, 893–900.
Oshiro, T., Sasaki, T., Nara, M., Tamada, T., Shimura, S., Maruyama, Y., Shirato, K., 2000. Suppression of maxi-K channel and membrane depolarization by synthetic polycations in single tracheal myocytes. Am. J. Respir. Cell Mol. Biol. 22, 528–534.
Osipchuk, Y., Cahalan, M., 1992. Cell-to-cell spread of calcium signals mediated by ATP receptors in mast cells. Nature 359, 241–244.
Pelleg, A., Schulman, E.S., 2002. Adenosine 5′-triphosphate axis in obstructive airway diseases. Am. J. Ther. 9, 454–464.
Priel, A., Silberberg, S.D., 2004. Mechanism of ivermectin facilitation of human $P2X_4$ receptor channels. J. Gen. Physiol. 123, 281–293.
Ralevic, V., Burnstock, G., 1998. Receptors for purines and pyrimidines. Pharmacol. Rev. 50, 413–492.
Rogers, M., Dani, J.A., 1995. Comparison of quantitative calcium flux through NMDA, ATP, and ACh receptor channels. Biophys. J. 68, 501–506.
Shimura, S., Sasaki, T., Nagaki, M., Takishima, T., Shirato, K., 1994. Extracellular ATP regulation of feline tracheal submucosal gland secretion. Am. J. Physiol. Lung Cell. Mol. Physiol. 267, L159–L164.
Silberberg, S.D., Li, M., Swartz, K.J., 2007. Ivermectin interaction with transmembrane helices reveals widespread rearrangements during opening of P2X receptor channels. Neuron 54, 263–274.
Somlyo, A.P., Somlyo, A.V., 1994. Signal transduction and regulation in smooth muscle. Nature 372, 231–236.
Soto, F., Garcia-Guzman, M., Gomez-Hernandez, J.M., Hollmann, M., Karschin, C., Stühmer, W., 1996. $P2X_4$: an ATP-activated ionotropic receptor cloned from rat brain. Proc. Natl. Acad. Sci. U.S.A. 93, 3684–3688.
Tamada, T., Sasaki, T., Saitoh, H., Ohkawara, Y., Irokawa, T., Sasamori, K., Oshiro, T., Tamura, G., Shimura, S., Shirato, K., 2000. A novel function of thyrotropin as a potentiator of electrolyte secretion from the tracheal gland. Am. J. Respir. Cell Mol. Biol. 22, 566–573.
von Kugelgen, I., Wetter, A., 2000. Molecular pharmacology of P2Y-receptors. Naunyn Schmiedebergs Arch. Pharmacol. 362, 310–323.
Worley, J.F., Kotlikoff, M.I., 1990. Dihydropyridine-sensitive calcium channels in airway smooth muscle cell. Am. J. Physiol. Lung Cell. Mol. Physiol. 259, L468–L480.
Yeung, D., Kharidia, R., Brown, S.C., Górecki, D.C., 2004. Enhanced expression of the $P2X_4$ receptor in Duchenne muscular dystrophy correlates with macrophage invasion. Neurobiol. Dis. 15, 212–220.
Zhang, Y.H., Hancox, J.C., 2003. A novel, voltage-dependent nonselective cation current activated by insulin in guinea pig isolated ventricular myocytes. Circ. Res. 92, 765–768.

Activation of Toll-Like Receptor 3 Augments Myofibroblast Differentiation

Hisatoshi Sugiura[1], Tomohiro Ichikawa[1], Akira Koarai[1], Satoru Yanagisawa[1], Yoshiaki Minakata[1], Kazuto Matsunaga[1], Tsunahiko Hirano[1], Keiichiro Akamatsu[1], and Masakazu Ichinose[1]

[1]Third Department of Internal Medicine, Wakayama Medical University School of Medicine, Wakayama, Japan

Airway remodeling is observed in the airways of patients with asthma, and differentiation of fibroblasts to myofibroblasts plays a critical role in the progress of airway remodeling. Viral infection induces not only the disease development and exacerbations but also airway remodeling. The aim of this study was to evaluate whether the activation of Toll-like receptor 3 (TLR3) can affect the differentiation of fibroblasts to myofibroblasts and the extracellular matrix (ECM) protein production. Human fetal lung fibroblasts (HFL-1) and adult lung fibroblasts were treated with a synthetic double-stranded RNA, polyinosine-polycytidylic acid (poly[I:C]) and the expression of α-smooth muscle actin (α-SMA), a marker of myofibroblast differentiation, was evaluated. The release of transforming growth factor-β_1 (TGF-β_1) and ECM protein production were assessed. The effect of anti-TGF-β antibody on the α-SMA and ECM production was also assessed. Poly(I:C) significantly augmented the α-SMA expression ($P < 0.01$) and release of TGF-β_1 ($P < 0.01$) compared with control. Bafilomycin, an inhibitor of TLR3 signaling, diminished poly(I:C)-augmented TGF-β_1 release. Anti–TGF-β_1 antibody inhibited the poly(I:C)-augmented α-SMA expression. Poly(I:C) enhanced translocation of nuclear factor-kB (NF-κB) and interferon regulatory factor-3 (IRF-3) into the nucleus. Poly(I:C)-augmented TGF-β_1 release was almost completely blocked by NF-κB inhibitors, but not by silencing IRF-3. The production of fibronectin and collagen I expression were significantly increased by poly(I:C) ($P < 0.01$) and they were inhibited by anti–TGF-β antibody. These results suggest that activation of TLR3 can affect the differentiation to myofibroblasts and enhance ECM production via the NF-κB–TGF-β_1–dependent pathway.

Keywords: viral infection; transforming growth factor-β_1; nuclear factor-kappa B; airway remodeling; asthma

CLINICAL RELEVANCE

Activation of Toll-like receptor 3 by double-stranded RNA can affect the differentiation to myofibroblasts and enhanced extracellular matrix production that are related to the airway remodeling after viral-induced exacerbations in asthma via the NF-κB–TGF-β1–dependent pathway.

Double-stranded RNA (dsRNA) is produced by many viruses in the infected cells during replication (1). It has been reported that dsRNA stimulates innate immune responses through Toll-like receptor 3 (TLR3) among the TLRs (2, 3). When TLR3 is activated by dsRNA, both nuclear factor-kappa B (NF-κB) and interferon regulatory factor-3 (IRF-3) translocate to the nucleus (2). NF-κB promotes various kinds of proinflammatory cytokine expression, whereas activation of IRF-3 results in the expression of type I interferon (IFN) and IFN-inducible genes (2).

Viral infection has been reported to play a pivotal role in the development (4) and exacerbation (5) of bronchial asthma. Kotaniemi-Syrjähen and coworkers have shown that viral infection during the first 3 yr of life increases the prevalence of asthma (6). Nicholson and colleagues have shown that infection with rhinovirus and coronavirus induces acute exacerbations of asthma (7). Airway epithelial cells infected with rhinovirus (8) or respiratory syncytial virus (RSV) (9) secrete greater amounts of eosinophilic chemokines, including eotaxin (8) and RANTES (9). Recently, Niimi and coworkers showed that dsRNA enhanced the release of eotaxin-1/CCL-11 from human bronchial smooth muscle cells (10). Furthermore, dsRNA could enhance airway allergen sensitization in a murine asthmatic model (11). These results suggest that viral infection could be involved in the pathogenesis of asthma through the activation of TLR3. Several reports have shown that viral infection induced airway remodeling (12–14). Psarras and colleagues have shown that airway epithelial cells infected with rhinovirus secrete greater amounts of vascular endothelial growth factor (VEGF), which is thought to be related to neovasculization in remodeling airways (12). Walter and coworkers have shown that paramyxovirus infection induces a chronic asthma phenotype characterized by airway remodeling and persistent airway hyperreactivity (13). Although viral infection has been recognized to be involved in the airway remodeling in asthma (12–14), the role of TLR3 in the airway remodeling has not been elucidated yet.

Airway remodeling is related to increased severity and irreversible airflow limitation in asthma and often leads to refractoriness of the disease in spite of treatment with high doses of corticosteroids (15). The parenchymal cells of the airway, including epithelial cells, airway smooth muscles, endothelial cells, and fibroblasts are responsible for maintenance of the airway structure and are involved in the progression of airway remodeling (16). Among these parenchymal cells, the myofibroblast is a key player in the excessive deposition of extracellular matrix (ECM) protein including collagen I, III, V, fibronectin, and tenascin in the lamina reticularis of the basement membrane (17). We previously demonstrated that chronic exposure to antigen induced the differentiation of fibroblasts to myofibroblasts in the airways and lungs of sensitized mice (18). In fact, there were more myofibroblasts within the airway walls of patients with asthma, especially patients with refractory asthma, compared with healthy subjects (19), suggesting that the differentiation of fibroblasts to myofibroblasts is a key process in the airway remodeling of asthma. Generally, transforming growth factor-β_1 (TGF-β_1) is the most important mediator in facilitating the differentiation of fibroblasts to myofibroblasts (20). In fact, TGF-β_1 production is increased in the airways of patients with asthma (21). Although the differentiation of fibroblasts to myofibroblasts and TGF-β_1 production play a pivotal role in the process of airway remodeling observed in asthma, the effect of dsRNA on

(*Received in original form September 29, 2008 and in final form October 27, 2008*)

Correspondence and requests for reprints should be addressed to Masakazu Ichinose, M.D., Ph.D., Third Department of Internal Medicine, Wakayama Medical University School of Medicine, 811-1 Kimiidera, Wakayama, Wakayama 641-0012, Japan. E-mail: masakazu@wakayama-med.ac.jp

Am J Respir Cell Mol Biol Vol 40. pp 654–662, 2009
Originally Published in Press as DOI: 10.1165/rcmb.2008-0371OC on November 6, 2008
Internet address: www.atsjournals.org

the differentiation and TGF-β_1 release in human lung fibroblasts is still unknown.

The present study, therefore, was designed to determine, using human lung fibroblasts, the following: (*1*) whether dsRNA could affect the differentiation of lung fibroblasts to myofibroblasts; (*2*) whether dsRNA enhances the release of TGF-β_1 and ECM proteins including fibronectin and collagen I in human lung fibroblasts; and (*3*) what signal transduction through the activation of TLR3 modulates the differentiation of lung fibroblasts to myofibroblasts.

MATERIALS AND METHODS

Materials

Commercially available reagents were obtained as follows: anti–TGF-β_1 antibody, TGF-β_1, biotinylated anti–TGF-β_1 antibody, neutralizing anti–TGF-β antibody, goat polyclonal anti-TLR3 antibody, recombinant human TLR3, and anti-immunoglobulin (IgG) were from R&D Systems (Minneapolis, MN); polyinosine-polycytidylic acid (poly[I:C]) was from Amersham Biosciences (Piscataway, NJ); 3′,3′,5,5′-tetramethyl benzidine (TMB), propidium iodide (PI), monoclonal anti-human fibronectin antibody, polyclonal anti-human fibronectin antibody, mouse monoclonal anti–α-SMA antibody, mouse monoclonal anti–β-actin antibody, anti-rabbit IgG antibody, and anti-goat IgG antibody were from Sigma (St. Louis, MO); MG132 and caffeic acid phenethyl ester (CAPE) and nuclear factor-kappa B (NF-κB) inhibitors were from Calbiochem (La Jolla, CA); mouse monoclonal anti–NF-κB p65 antibody, rabbit polyclonal anti–IRF-3 antibody, and mouse monoclonal anti-lamin A/C antibody were from Santa Cruz Biotechnology (Santa Cruz, CA); Dulbecco's Modified Eagle's Medium (DMEM), fetal calf serum (FCS), and antibiotic-antimycotic were purchased from Invitrogen Life Technologies (Grand Island, NY).

Cell Culture

Human fetal lung fibroblasts (HFL-1) were obtained from the American Type Culture Collection (Rockville, MD). Three strains of adult lung fibroblasts were obtained from lung tissues resected by surgical operation from the patients with lung cancer and purchased from Takara Bio, Inc. (Ohtsu, Siga, Japan). The study was conducted with the approval of the Wakayama Medical University Committee on Clinical Investigation. Written informed consent was obtained from all subjects. The HFL-1 and adult cells were cultured on tissue culture dishes with DMEM supplemented with 10% FCS, 100 μg/ml penicillin, 250 μg/ml streptomycin, and 2.5 μg/ml fungizone. Cells were cultured at 37°C in a humidified atmosphere of 5% CO_2 and passaged. HFL-1 cells were used between the 14th and 18th passages. The adult fibroblasts were used between the 3rd and 7th passages. To evaluate the mediator production in a monolayer culture, cells were seeded in 6-well tissue culture plates at a cell density of 1×10^5 /ml. At 90% confluence, cells were treated with various concentrations of poly(I:C) in serum-free DMEM (SF-DMEM). For the investigation of the effect of neutralizing anti–TGF-β antibody on poly(I:C)-mediated mediator release, anti–TGF-β antibody (10 μg/ml) was also added to the media 30 minutes before the treatment with poly(I:C). The supernatants were harvested after 48 hours of treatment with poly(I:C) and stored at −80°C until later assay.

Immunochemical Localization of TLR3, NF-κB p65, and IRF-3

HFL-1 cells were seeded in 8-well chamber slides at a density of 1×10^5 /ml and cultured for 24 hours, and then the medium was replaced with SF-DMEM for 24 hours. The cells were incubated with 10 μg/ml poly(I:C) for the staining of NF-κB p65 and IRF-3. After washing, the slides were fixed with freshly prepared 4% paraformaldehyde in PBS for 30 minutes at room temperature and then were blocked with blocking reagent (Dako, Kyoto, Japan) for 1 hour at room temperature and rinsed. The cells were incubated with goat polyclonal anti-TLR3 antibody (10 μg/ml) or goat IgG as a negative control for immunostaining of TLR3. The cells were also incubated with mouse monoclonal anti–NF-κB p65 antibody (1:100 dilution) or rabbit polyclonal anti–IRF-3 antibody (1:100 dilution) at 4°C overnight. After washing, cells were incubated with the appropriate FITC-conjugated secondary antibodies (1:1,000 dilution; Sigma) for 60 minutes at room temperature. The cells were viewed by epifluorescence microscopy (E-800; Nikon) and photographed with a digital camera (DMX-1200C; Nikon) under ×400 magnification.

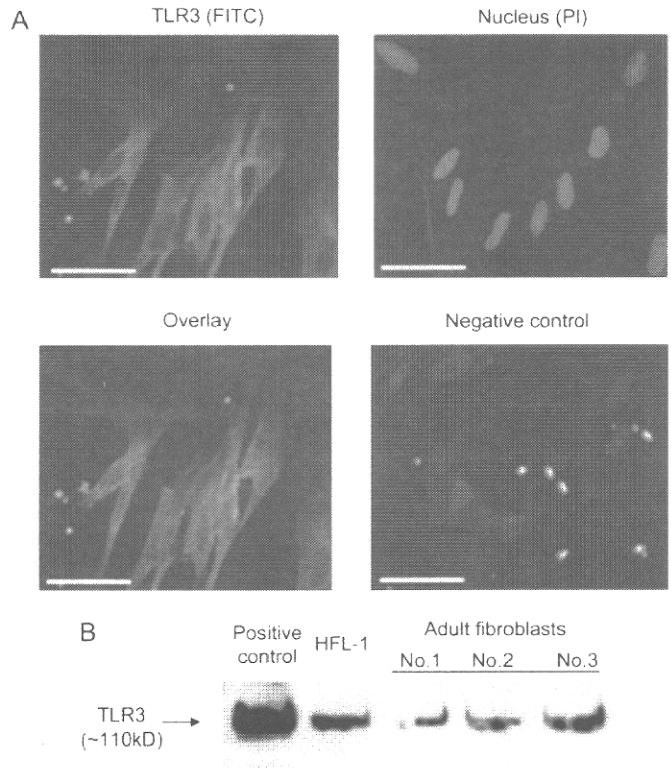

Figure 1. Detection of Toll-like receptor3 (TLR3) in human fetal lung fibroblasts (HFL-1) and adult lung fibroblasts by immunostaining and immunoblotting. (*A*) The localization of TLR3 in HFL-1 cells was investigated by immunostaining. Shown are representative photographs of the immunoreactivity of TLR3 (*upper left panel, green*), immunofluorescence of the nucleus (*upper right panel, red*), an overlaid image (*lower left panel, green* and *red*), and a negative control (*lower right panel, red*). (*B*) TLR3 in HFL-1 and three different strains of normal adult lung fibroblasts (Nos. 1–3) were also detected by immunoblotting. Human recombinant TLR3 was used as a positive control. PI, propidium iodide. *Scale bars* = 100 μm.

Western Blotting

Cells were seeded in 60-mm dishes at a density of 1×10^5/ml. At 90% confluence, the cells were starved with SF-DMEM for 24 hours in the case of α-SMA expression. Then, the cells were treated with various concentrations of poly(I:C) in the presence or absence of bafilomycin, MG132, or neutralizing anti–TGF-β antibody for 48 hours. The cells were washed with ice-cold PBS and homogenized in cell lysis buffer. To obtain the nuclear and cytosolic fractions, a Nuclear Extraction Kit (Active Motif, Carlsbad, CA) was used according to the manufacturer's instruction. Equal amounts of protein were loaded and separated by electrophoresis on 12.5% SDS polyacrylamide gels. After electrophoresis, the separated proteins were transferred to a PVDF membrane (Bio-Rad Laboratories, Hercules, CA). The following antibodies were used for detection of the target proteins: goat polyclonal anti-TLR3 antibody (0.2 μg/ml; R&D Systems), mouse monoclonal anti–α-SMA antibody (1:5,000 dilution), mouse monoclonal anti–β-actin antibody (1:10,000 dilution), mouse monoclonal anti–NF-κB p65 antibody (1:200 dilution), rabbit polyclonal anti–IRF-3 antibody (1:500 dilution),

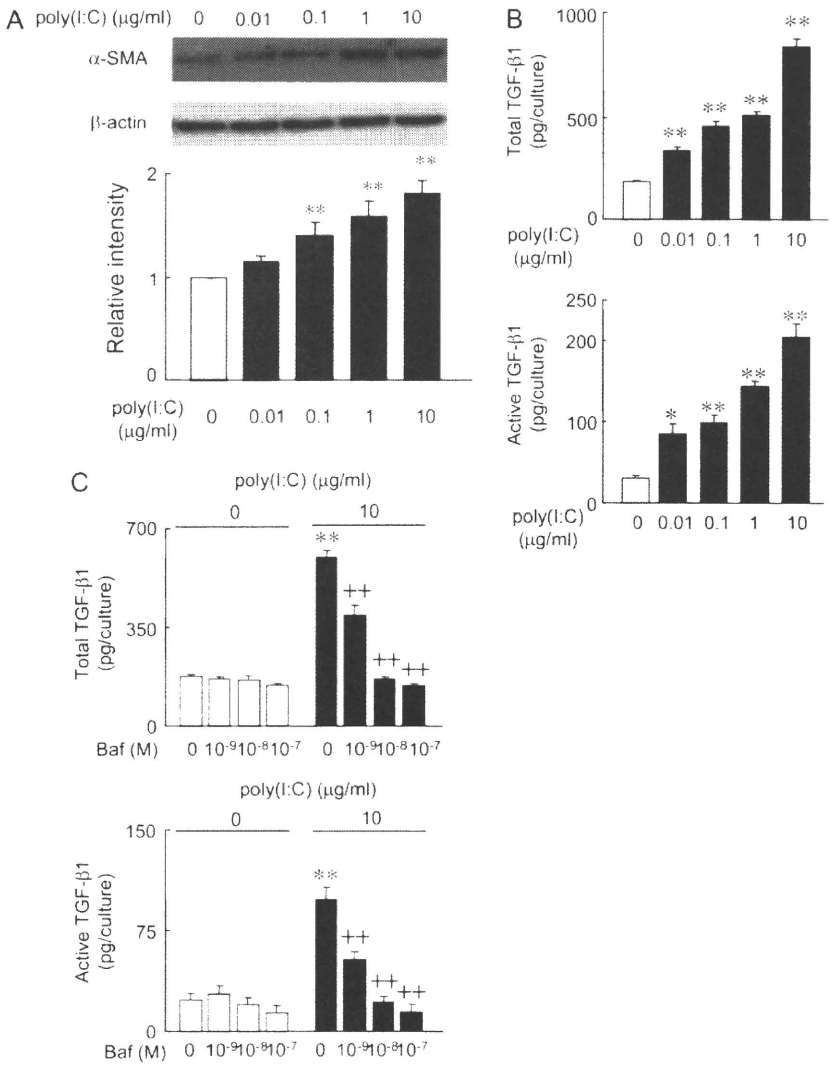

Figure 2. Effect of polyinosine-polycytidylic acid (poly[I:C]) on α-smooth muscle actin (α-SMA) expression and TGF-β_1 release, and effect of bafilomycin on the poly(I:C)-augmented TGF-β_1 release by HFL-1 cells. Fibroblasts were prepared in a monolayer culture, exposed to various concentrations of poly(I:C), a synthetic double-stranded RNA (dsRNA) and the cell lysates were harvested. (*A*) α-SMA expression was assessed by immunoblotting. Each band intensity was assessed by densitometry. Relative intensity was calculated by dividing each α-SMA band intensity by each appropriate β-actin band intensity. All values are mean ± SEM for six separate experiments. Fibroblasts were also treated with various concentrations of poly(I:C) in the (*B*) absence or (*C*) presence of various concentrations of bafilomycin, an inhibitor of endosomal acidification. After 48 hours, media were harvested and assayed for TGF-β_1 by enzyme-linked immunosorbent assay (ELISA). Total TGF-β_1 (*upper panels*) and active form of TGF-β_1 (*lower panels*) were measured. All values are mean ± SEM for four to eight separate experiments, each performed in duplicate. $^*P < 0.05$, $^{**}P < 0.01$ compared with the values of control; $++P < 0.01$ compared with the values of vehicle-pretreated poly(I:C)-treated group. Baf, bafilomycin.

mouse monoclonal anti-lamin A/C antibody (1:400 dilution), or rabbit polyclonal anti-collagen I antibody (1:5,000 dilution; Rockland Immunochemicals, Gilbertsville, PA). Bound antibodies were visualized using the appropriate peroxidase-conjugated secondary antibodies and enhanced chemiluminescence (Amersham Biosciences, Buckinghamshire, UK) with a chemiluminescene imaging system (Luminocapture AE6955; Atto Co., Tokyo, Japan). Band intensity was quantified by densitometry (Image J; NIH, Frederick, MD).

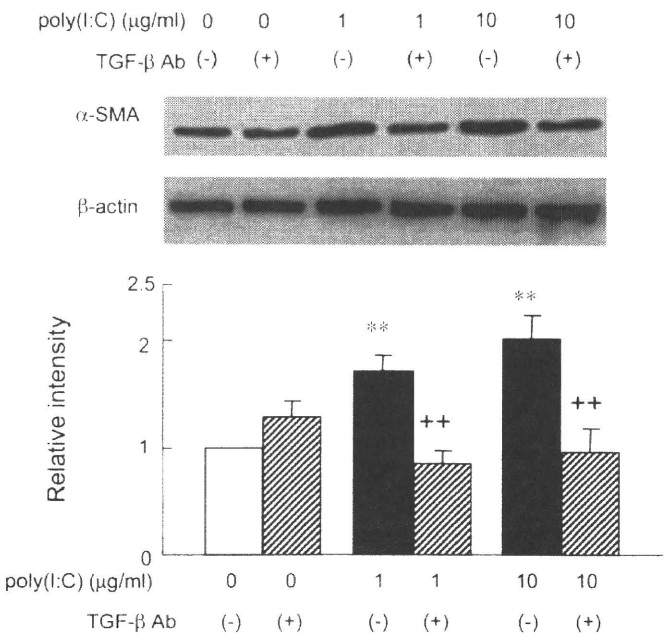

Figure 3. Effect of neutralizing anti–TGF-β antibody on the poly(I:C)-augmented α-SMA expression. Fibroblasts were treated with various concentrations of poly(I:C) in the presence of neutralizing anti–TGF-β antibody or control IgG, and cell lysates were obtained. α-SMA expression was assessed by immunoblotting. Each band intensity was assessed by densitometry. Relative intensity was calculated by dividing each band intensity of α-SMA by each appropriate β-actin band intensity. All values are mean ± SEM for four to eight separate experiments. $^{**}P < 0.01$ compared with the values of the control; $++P < 0.01$ compared with the values of the control IgG-pretreated poly(I:C)-treated group.

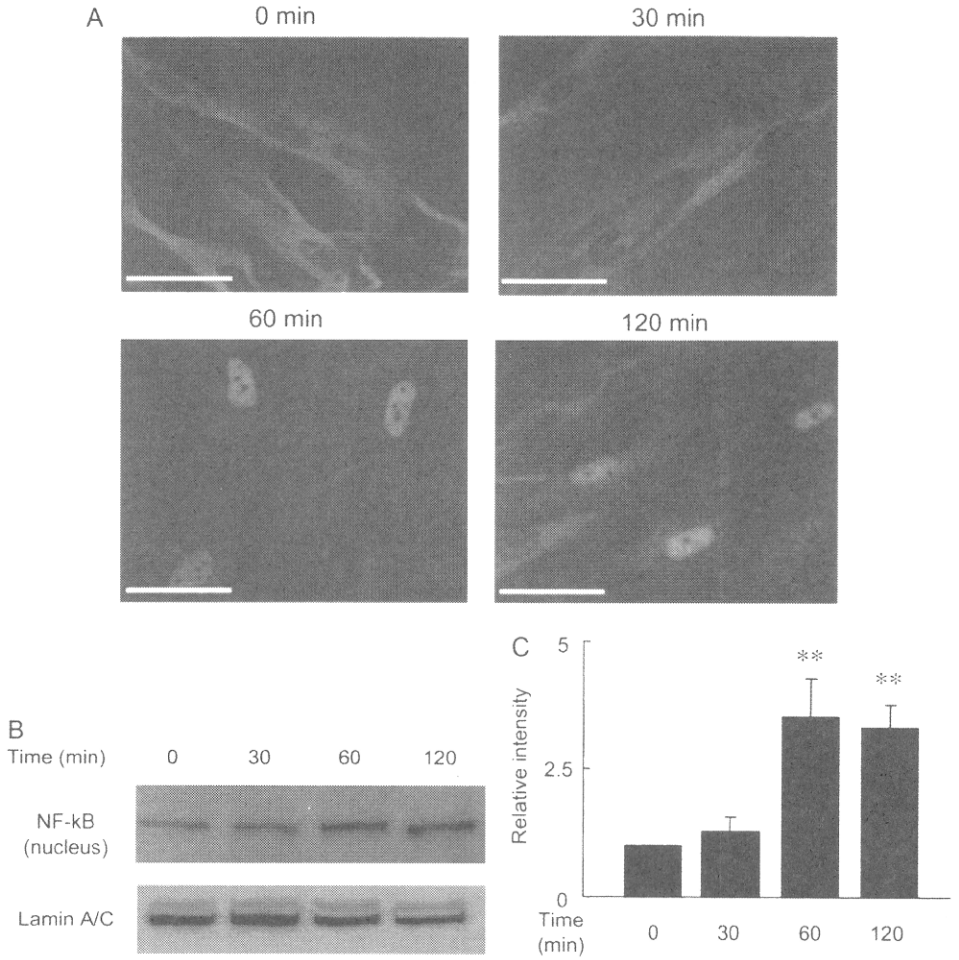

Figure 4. Effect of poly(I:C) on translocation of nuclear factor-kappa B (NF-κB) p65 into the nucleus in HFL-1 cells. Cells were treated with 10 μg/ml poly(I:C) in various time courses and the nuclear fraction of the cell lysate was obtained for immunoblotting. Translocation of NF-κB p65 into the nucleus was evaluated by both (*A*) immunocytochemistry and (*B*) immunoblotting. Each band intensity was assessed by densitometry. (*C*) Relative intensity was calculated by dividing each NF-κB band intensity by each appropriate lamin A/C band intensity. All values are mean ± SEM for four separate experiments. $^{**}P < 0.01$ compared with the values of control. *Scale bars* = 100 μm.

Measurement of TGF-β_1, Fibronectin, and IFN-β

TGF-β_1 and fibronectin in the media were determined by enzyme-lnked immunosobent assay (ELISA) (21). Briefly, the quantification of TGF-β_1 was performed as follows. Plates were coated with monoclonal anti–TGF-β_1 antibody at 4°C overnight. After being washed three times, standards and samples were added and incubated at room temperature for 2 hours. To measure TGF-β_1, all samples were assayed both with and without acidification and neutralization to convert the latent form of TGF-β_1 to the active form. To accomplish this, a 500-μl sample was mixed with 100 μl of 1 N HCl and, after 10 minutes at room temperature, neutralized with 100 μl of 1.2 N NaOH/0.5 M N-2-hydroxyethylpiperazine-N′-ethanesulphonic acid. To measure the active form of TGF-β_1, the samples were concentrated approximately 5 to 10 times by Ultrafree-MC (Millipore Corporation, Bedford, MA). Bound antigen was detected after adding biotinylated anti–TGF-β_1 antibody for 1 hour at room temperature. After being washed, horseradish peroxidase (HRP)-streptavidin (1:20,000 dilution) was then added for 1 hour. Bound HRP was detected with TMB. The reaction was stopped with 1 M H_2SO_4, and the product was quantified at 450 nm with a microreader. Fibronectin was assayed with an ELISA that specifically detects human but not bovine fibronectin (22). Plates were coated with monoclonal anti-fibronectin antibody at 4°C overnight. After being washed, standards and samples were added and incubated at room temperature for 2 hours. After being washed again, bound antigen was detected after adding polyclonal anti-human fibronectin antibody (1:2,000 dilution) at room temperature for 1 hour. HRP-conjugated anti-rabbit IgG antibody (1:10,000 dilution) was added at room temperature for 1 hour. Bound HRP was detected with TMB. The reaction was stopped with 1 M H_2SO_4, and the product was quantified at 450 nm with a microreader. IFN-β in the media was also measured by an ELISA kit (Thermo Scientific Inc., Rockford, IL) according to the manufacturer's protocol.

IRF-3 Silencing

Cells were seeded in 100-mm dishes in DMEM with 10% FCS. At 50% confluence, transfection with siRNA was performed. In one tube, 40 μl of lipofectamine 2000 (Invitrogen Life Technologies) was mixed gently with 1.5 ml Opti-MEM medium (Invitrogen Life Technologies) and incubated for 5 minutes at room temperature. In a separate tube, 975 pmol of either nontargeting or IRF-3 siRNA (SMART pool plus; Dharmacon, Lafayette, CO) were mixed gently with 1.5 ml Opti-MEM medium. These siRNA and lipofectamine solutions were then combined, gently mixed, and incubated for 20 minutes at room temperature. After incubation, 2 ml of DMEM without FCS and antibiotics were added to obtain a final volume of 5 ml (final concentration of siRNAs = 200 nM), which was added to each dish. The cells were then incubated at 37°C for 6 hours. Five milliliters of DMEM with 20% FCS were then added to obtain a final volume of 10 ml of DMEM with 10% FCS for each dish, and the cells were further incubated at 37°C for 18 hours. After that, media were changed to DMEM with 10% FCS and further cultured for 24 hours. The siRNA-treated cells were then used to assess the role of IRF-3 on TGF-β_1 release in the presence of 10 μg/ml poly(I:C) or to assess IRF-3 expression by immunoblotting.

Statistical Analysis

Data were expressed as means ± SEM. Experiments with multiple comparisons were evaluated by one way ANOVA followed by Bonferroni's test or Scheffé's test to adjust for multiple comparisons. In cases of different sample numbers among the experimental groups, we used Scheffé's test as a *post hoc* test. In other cases, Bonferroni's test was used. An unpaired two-tailed Student's *t* test was used for single comparisons. Probability values of less than 0.05 were considered significant.

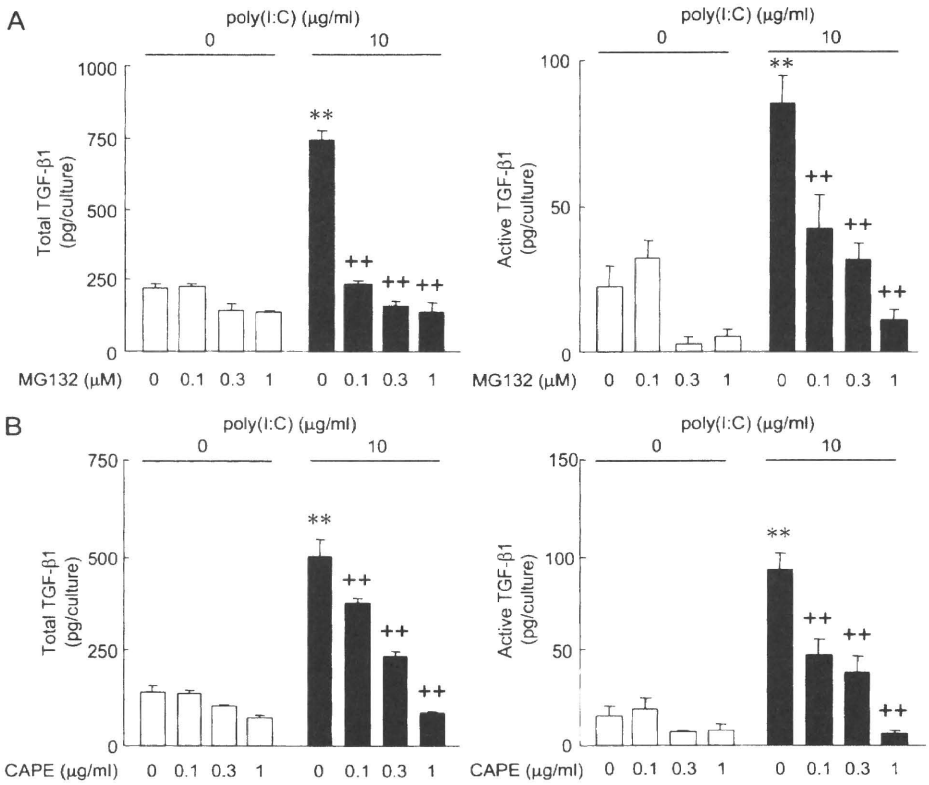

Figure 5. Effect of MG132 and caffeic acid phenethyl ester (CAPE), novel NF-κB inhibitors, on the poly(I:C)-augmented TGF-β_1 release. Fibroblasts were treated with poly(I:C) in the presence or absence of various concentrations of (*A*) MG132 and (*B*) CAPE. After 48 hours, media were harvested and assayed for TGF-β_1 by ELISA. Total TGF-β_1 (*left panels*) and active form of TGF-β_1 (*right panels*) were measured. All values are mean ± SEM for four to eight separate experiments, each performed in duplicate. $^{**}P < 0.01$ compared with the values of control; $++P < 0.01$ compared with the values of vehicle-pretreated poly(I:C)-treated group.

RESULTS

To determine whether human fetal lung fibroblasts and normal adult lung fibroblasts express TLR3, we investigated the expression of TLR3 in HFL-1 and normal adult cells. As shown in Figure 1A, TLR3 was detected by immunochemistry. To confirm this, we performed immunoblotting against TLR3. The TLR3 in HFL-1 cells and three different strains of normal adult lung fibroblasts were detected at approximately 110 kD as previously reported (Figure 1B).

To investigate whether poly(I:C) induces the differentiation of fibroblasts to myofibroblasts, we assessed the expression of α-SMA by treatment with various concentrations of a synthetic double-stranded RNA, poly(I:C). Poly(I:C) significantly augmented α-SMA expression in a concentration-dependent manner (at 10 μg/ml, 1.75 ± 0.13-fold increase, $P < 0.01$; Figure 2A). Because TGF-β_1 is the most important mediator for the differentiation to myofibroblasts, we investigated whether poly(I:C) augments TGF-β_1 release by HFL-1 cells. Poly(I:C) significantly increased total TGF-β_1 (at 10 μg/ml, 840 ± 40 versus 177 ± 9.3 pg/culture, $P < 0.01$; Figure 2B, *upper panel*) and active TGF-β_1 release (at 10 μg/ml, 204 ± 16 versus 30.7 ± 2.6 pg/culture, $P < 0.01$; Figure 2B, *lower panel*) in a concentration-dependent manner. To confirm the effect of poly(I:C) on the TGF-β_1 release, we treated the cells with bafilomycin, which is an inhibitor of endosomal acidification, to block the TLR3 signal transduction. As shown in Figure 2C, bafilomycin diminished the effects of poly(I:C) on total TGF-β_1 (at 10^{-7} M, 144 ± 6.8 versus 601 ± 23 pg/culture, $P < 0.01$, *upper panel*) and active TGF-β_1 release (at 10^{-7} M, 97.5 ± 9.3 versus 14.5 ± 5.2 pg/culture, $P < 0.01$, *lower panel*). To clarify the mechanistic role of TGF-β_1 in the poly(I:C)-augmented α-SMA expression, we investigated the effect of neutralizing anti–TGF-β antibody on the α-SMA expression. Neutralizing anti–TGF-β antibody almost completely inhibited the poly(I:C)-augmented α-SMA expression compared with the control IgG-treated group (at 10 μg/ml, 0.958 ± 0.23 versus 2.02 ± 0.20-fold increase, $P < 0.01$; Figure 3).

To investigate how poly(I:C) augments the TGF-β_1 release, we assessed the translocation of NF-κB into the nucleus because NF-κB is thought to regulate TGF-β_1 expression. The translocation of NF-κB p65 into the nucleus was assessed by immunostaining and immunoblotting. After treatment with 10 μg/ml poly(I:C), the translocation NF-κB p65 was increased at 60 minutes and the fluorescence intensity of NF-κB p65 in the nucleus persisted until 120 minutes (Figure 4A). The amount of NF-κB p65 in the nuclear fraction at 60 minutes was significantly increased compared with control (3.53 ± 0.76-fold increase, $P < 0.01$; Figures 4B and 4C). To investigate whether NF-κB is involved in the fibroblast-mediated TGF-β_1 release, the effect of MG132 and CAPE, NF-κB inhibitors, on the TGF-β_1 release was evaluated. As shown in Figure 5A, MG132 significantly inhibited the poly(I:C)-augmented total TGF-β_1 (at 1 μM, 742 ± 35 versus 135 ± 35 pg/culture, $P < 0.01$, left panel) and active TGF-β_1 release (at 1 μM, 85.8 ± 9.0 versus 10.9 ± 3.4 pg/culture, $P < 0.01$, right panel) as well as CAPE (Figure 5B).

After activation of TLR3, IRF-3 signaling was enhanced as well as NF-κB in other types of cells; therefore, we investigated the role of IRF-3 on the fibroblast-mediated TGF-β_1 release. After treatment with 10 μg/ml poly(I:C), the translocation of IRF-3 was enhanced at 60 minutes and the fluorescence intensity of IRF-3 in the nucleus persisted until 120 minutes (Figure 6A). The amount of IRF-3 in the nuclear fraction at 60 minutes was significantly increased compared with control (Figure 6B). To investigate whether IRF-3 is involved in the fibroblast-mediated TGF-β_1 release, the effect of silencing IRF-3 on TGF-β_1 release was evaluated. IRF-3 siRNA diminished the expression of IRF-3 compared with the nontargeting siRNA–treated group (Figure 6C). To confirm whether IRF-3 siRNA can inhibit the IRF-3 signaling, we investigated the effect of siRNA on the IFN-β release. Ten micrograms per

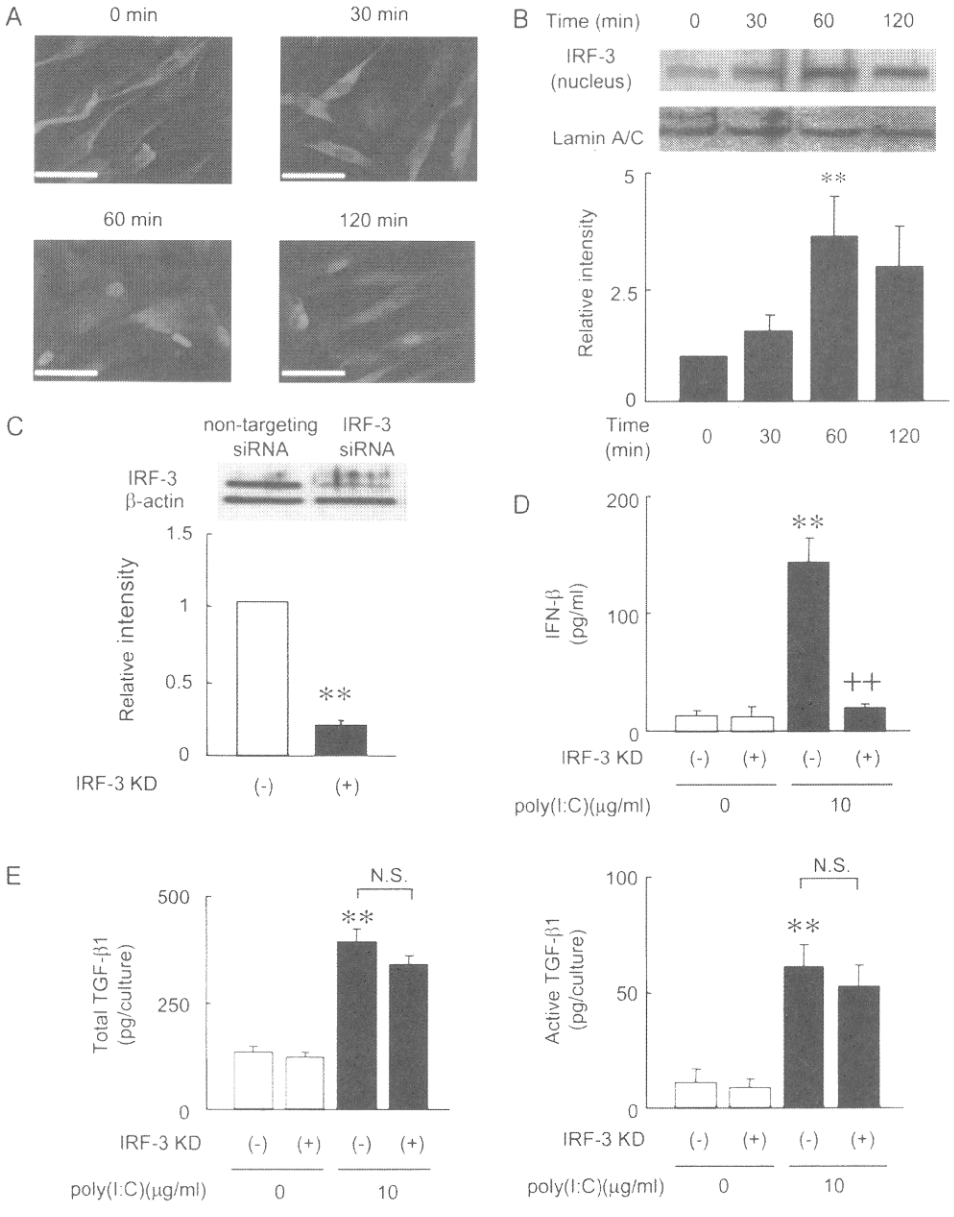

Figure 6. Effect of poly(I:C) on translocation of interferon regulatory factor-3 (IRF-3) into the nucleus in HFL-1 cells and effect of IRF-3 silencing with siRNA on the poly(I:C)-augmented interferon (IFN)-β and TGF-β_1 release. Cells were treated with 10 μg/ml poly(I:C) in various time courses and the nuclear fraction of the cell lysate was obtained for immunoblotting. Translocation of IRF-3 into nucleus was evaluated by both (*A*) immunocytochemistry and (*B*) immunoblotting. Each band intensity was assessed by densitometry. Relative intensity was calculated by dividing each IRF-3 band intensity by each appropriate lamin A/C band intensity. Cells were also treated with nontargeting control or IRF-3 siRNA for 24 hours. Cells were further incubated with or without poly(I:C) for 48 hours. Media were harvested and assayed for IFN-β and TGF-β_1 by ELISA. (*C*) Expression of IRF-3 was detected at approximately 50 kD by immunoblotting. The expression was assessed by densitometry. Relative intensity was calculated by dividing each IRF-3 band intensity by each appropriate β-actin band intensity. Effect of IRF-3 silencing on (*D*) IFN-β and (*E*) TGF-β_1 release was assessed by ELISA. All values are mean ± SEM for four separate experiments. $^{**}P < 0.01$ compared with the values of control. IRF-3, interferon regulatory factor-3; IRF-3 KD, IRF-3 knock down; N.S., not significant. *Scale bars* = 100 μm.

milliliter of poly(I:C) significantly augmented IFN-β release compared with control (Figure 6D), and silencing IRF-3 significantly inhibited the IFN-β release (Figure 6D). There was no effect of silencing on either total TGF-β_1 (Figure 6E, *left panel*) or active TGF-β_1 release (Figure 6E, *right panel*).

We also investigated the effects of poly(I:C) on the ECM protein production. Poly(I:C) significantly augmented the release of fibronectin in a concentration-dependent manner (at 10 μg/ml, 4,900 ± 264 ng/ml versus 1,288 ± 342 ng/ml, $P < 0.01$; Figure 7A). Poly(I:C) also significantly augmented the expression of collagen I in a concentration-dependent manner (at 10 μg/ml, 2.59 ± 0.27-fold increase, $P < 0.01$; Figure 7B). Neutralizing anti–TGF-β antibody significantly inhibited the poly(I:C)-augmented fibronectin release compared with the control IgG-treated group (at 10 μg/ml, 4,391 ± 96.9 versus 2,422 ± 52.5 ng/ml, $P < 0.01$; Figure 7C). The poly(I:C)-augmented collagen I expression was also significantly inhibited by neutralizing anti–TGF-β antibody compared with the control IgG-treated group (at 10 μg/ml, 3.11 ± 0.38 versus 1.10 ± 0.24-fold increase, $P < 0.01$; Figure 7D).

Some of the data shown in HFL-1 cells were also investigated in normal adult lung fibroblasts. Poly(I:C) significantly augmented the α-SMA expression, release of TGF-β_1 and fibronectin, and collagen I expression in adult lung fibroblasts (Table 1).

DISCUSSION

The present study demonstrated that a synthetic double-stranded RNA, poly(I:C) significantly augmented α-SMA expression in HFL-1 cells, indicating that the activation of TLR3 stimulates the differentiation of fibroblasts to myofibroblasts. Poly(I:C) also enhanced the TGF-β_1 release and treatment with anti–TGF-β_1 antibody inhibited the poly(I:C)-augmented α-SMA expression. Poly(I:C) promoted the translocation of NF-κB p65 and IRF-3 into the nucleus in human lung fibroblasts as well as other types of cells. The poly(I:C)-augmented TGF-β_1 release was regulated by NF-κB, but not by IRF-3. In addition, fibronectin and collagen I production were significantly enhanced by poly(I:C) and were inhibited by anti–TGF-β anti-